Fundamental limits of pulsed quantum light spectroscopy of a two-level atom

Evangelia Bisketzi,[1] Aiman Khan,[1] Francesco Albarelli,[2,*] and Animesh Datta[1]

[1] *Department of Physics, University of Warwick, Coventry, CV4 7AL, United Kingdom*
[2] *Dipartimento di Fisica "Aldo Pontremoli", Università degli Studi di Milano, via Celoria 16, 20133 Milan, Italy*

(Dated: June 30, 2022)

Quantum light spectroscopy is an emerging field in which the quantum nature of light is exploited to reveal information about the properties of matter. Although there is evidence that spectroscopy with quantum light can improve upon classical light, this advantage has not been rigorously assessed. Instead of a standard spectroscopic analysis, we use quantum estimation theory to study the ultimate precision limit for the estimation of parameters of the matter system, when it is probed by a travelling pulse of quantum light. Concretely, we focus on the estimation of the interaction strength between the pulse and a two-level atom, equivalent to the estimation of the dipole moment. We present a detailed analysis of single-photon pulses, which we use to highlight the interplay between the information gained from the photon absorption by the atom, as measured in absorption spectroscopy, and the perturbation to the field temporal mode due to spontaneous emission. Going beyond the single-photon regime, we introduce an approximate model to study more general states of light in the limit of short pulses, where spontaneous emission can be neglected. We also show that for a vast class of entangled biphoton states entanglemment gives no fundamental advantage and the same precision can be obtained with a separable state. We conclude by applying the theoretical results to study a concrete problem, dipole-moment estimation of a sodium atom.

I. INTRODUCTION

[The introduction needs to be shortened]

Spectroscopy seeks to estimate one or more parameters appearing in the model of a matter system by measuring the light that has interacted with it.

Recent technological developments have made it possible to use quantum light, i.e. Fock, squeezed or entangled states of light, in spectroscopy [1]. This resulted in enhanced sensing to better precisions than the classical shot noise limit [2], in obtaining different scaling of the spectroscopic signals [3] and in new spectroscopic techniques [4, 5]. However, the advantages of using entangled light in spectroscopy remain unclear.

Many proposals. Nothing quantitative. Quantitative evaluation of the performance of quantum light - precision. Absorption spectroscopy - linear at short time (this paper), nonlinear at long time (next paper).

In this paper, we start to uncover the fundamental limits of quantum spectroscopy by employing quantum estimation theory and ideas from quantum metrology. This approach is needed to understand to what extent the enhancements of quantum metrology [6, 7] are relevant under the more stringent and practical constraints of quantum light spectroscopy experiments.

More concretely, we focus on a paradigmatic scenario that can be considered a minimal example of quantum spectroscopy: a pulse of quantum light is used to probe a single two-level atom. In paricular, we study the quantum limits to the precision of estimating the interaction parameter Γ between the pulse and the atom, proportional to the square of the EDM (thus the two estimation tasks are essentially equivalent). Even for such a simple two-level quantum system the dynamics is not trivial and the problem presents a rich phenomenology.

When a propagating pulse of quantized radiation interacts with an atom or molecule, a photon from the incoming pulse is absorbed and induce an excitation, but at the same time the excited state tends to decay due to spontaneous emission. Indeed, if the atom is perfectly coupled only to the spatial and polarization mode of the incoming pulse it cannot emit into other modes and, after the pulse has passed, Γ can be interpreted as the decay rate. The spontaneously emitted light has the well-known exponentially decaying shape in time, thus the light after the interaction will have a different shape, as well as a different quantum state. Perfect coupling can be achieved even in free space by careful mode-matching [8, 9]; however, in spectroscopy the pulse mode usually represents a propagating paraxial beam and thus the spontaneous emission does not happen exclusively into the pulse mode, but also in other orthogonal spatial modes with an overall rate $\Gamma_\perp$.

By studying the case of single-photon pulses in detail we separate two sources of information about the parameter Γ: an absorption contribution, reminiscent of absorption spectroscopy with single-photon states [10], and a temporal-shape perturbation contribution, reminiscent of fluorescence lifetime estimation [11] and fluorescence spectroscopy [12]. These phenomena are usually studied in separate frameworks, but the underlying physical model of light-matter interaction contains both absorption and emission contributions, thus we treat the problem in a unified manner, using the lens of quantum estimation theory.

When light is used to probe an ensemble of atoms, quantum spectroscopy strategies that take into account also the phase shift and not only absorption have been

* francesco.albarelli@gmail.com

studied [13, 14], as well as quantum strategies for absorption measurements taking into account the saturation [15]. We take a very different approach by studying the exact dynamics of a pulse interacting with a *single* atom. Fluorescence lifetime estimation is also closely related to our problem, but in that context one simply assumes that the atom is initially excited and measures the spontaneously emitted light [11]. We consider instead the atom initially in the ground state and model also the excitation induced by a quantum pulse of light.

If the pulse of radiation is much shorter than the spontaneous emission lifetime of the relevant transition, there is a clear separation of time scales: absorption and spontaneous emission can be considered as two distinct phenonema that happen one after the other. In this regime of short pulses, we can essentially neglect spontaneous emission. We employ this simplification to study more general quantum states of light and we argue that this regime is also appropriate to study free space configurations, because the additional decay dictated by $\Gamma_\perp$ is predominant and prevents further information to be encoded in the pulse spatial mode.

Regarding entangled light, previous works have shown that for one-photon processes the statistics obtained from an entangled photon pair can be reproduced with correlated separable states [16], as long as the photons are measured individually and do not interact again after passing through the sample. Here, we show that for a large class of biphoton states this kind of measurements is optimal and thus there is no fundamental advantage due to entanglement. We also show that for such entangled biphoton states the precision can always be improved by probing the atom with an appropriate single-photon wavepacket. This is in perfect agreement with the case of absorption spectroscopy, where the ultimate precision limit is achieved by using single-photon states [17], with correlated pairs only approaching that limit [10, 15, 18].

Matter/atom?

Finally, we study a concrete example of a sodium atom in free space. We show that a one-photon Gaussian wavepacket and the entangled photon pair with Gaussian joint spectral amplitude have similar performances, while the performance of coherent states is much worse. Moreover the performance of the entangled photon pair is decreased for more entangled states. Overall, our results indicate that using Fock states to estimate the EDM of a two-level atom is preferable to using entangled light, similarly to the case of absorption measurements.

Our main results are as follows:

1. Exc. prob. and QFI different

2. CFI = QFI/2 for incoming pulse measurement.

The paper is structured as follows. In Sec. II we present our theoretical framework: the model, the methods to solve the dynamics, and a summary of local quantum estimation theory that we use for our analysis. In Sec. III we present an extensive analysis of the problem for single-photon pulses, where analytical or semi-analytical solution are available. In Sec. IV we show how to approximate the problem to a much simpler one in the regime of short pulses and present general solution within this approximation. In Sec. V we present some general remarks about entangled biphoton states for this estimation problem. In Sec. VI we apply our general results a concrete application: dipole-moment estimation with a sodium atom. We conclude the paper with Sec. VII where we summarize and discuss our results.

II. THEORETICAL FRAMEWORK

We begin with the theoretical model of light-atom interaction, followed by the analytical and numerical methods to solve the dynamics in various regimes. We then provide a brief introduction to quantum estimation theory, needed to quantify the achievable precision.

A. Model

1. *Atom, field, and their iinteraction*

We consider a single two-level atom (the "atom" subsystem) modelled by its free Hamiltonians H_A. The ground and excited states of the atom are denoted by $|g\rangle$ and $|e\rangle$ respectively. Setting the ground state energy to zero,

$$H_\mathrm{A} = \hbar\omega_0 |e\rangle\langle e|, \tag{1}$$

where ω_0 is the transition frequency. We assume the atom, for simplicity, to be stationary in free space.

We next consider a travelling pulse of quantized radiation field (the "field"/ pulse? subsystem) modelled by its free Hamiltonians H_F. A travelling pulse must be described by a continuum of frequencies. As is customary in spectroscopic setups, we assume the field to have a well-defined direction of propagation. This leads to the free field Hamiltonian [19]

$$H_\mathrm{F} = \hbar \int_0^\infty d\omega\ \omega a^\dagger(\omega) a(\omega), \tag{2}$$

with the bosonic operators $[a(\omega), a^\dagger(\omega)] = \delta(\omega - \omega')$ indexed by a continuous frequency ω. We further assume the field to be sufficiently narrowband around a carrier frequency $\bar{\omega}$. Then the positive-frequency component of the electric field operator (in the interaction picture with respect to the free Hamiltonian) is

$$\mathbf{E}(t) = \mathrm{i}\hbar\boldsymbol{\epsilon}\mathcal{A}(\bar{\omega}) \int_{-\infty}^\infty d\omega\ a(\omega) \mathrm{e}^{-i\omega t}, \tag{3}$$

where $\boldsymbol{\epsilon}$ is a unit polarization vector, $\mathcal{A}(\bar{\omega}) = \sqrt{\bar{\omega}/(4\pi\epsilon_0 c A\hbar)}$ and A is the transverse quantisation area.

The interaction the travelling pulse and the atom is illustrated in Fig. 1. It is modelled by an interaction term H_I. As the atom is much smaller than typical optical

wavelengths, the interaction is captured by the dipole approximation. Making next the rotating wave approximation, the interaction Hamiltonian in the interaction picture takes the standard form [20]

$$H_{\rm I}(t) = \mathbf{d}(t)\cdot\mathbf{E}^{\dagger}(t) + \mathbf{d}^{\dagger}(t)\cdot\mathbf{E}(t), \tag{4}$$

$$= -\mathrm{i}\hbar\sqrt{\Gamma}\big(\sigma_+ a(t) - \sigma_- a^{\dagger}(t)\big) \tag{5}$$

where $\mathbf{d}(t) = \boldsymbol{\mu}_{eg}\sigma_- e^{-\mathrm{i}\omega_0 t}$ is the positive frequency part of the dipole operator, $\boldsymbol{\mu}_{eg} = -q_e\langle e|\mathbf{r}|g\rangle$ is the relevant dipole matrix element (q_e is the charge of the electron), and $\sigma_- = |g\rangle\langle e| = \sigma_+^{\dagger}$. In (5) we have introduced the so-called "quantum white-noise" operators [1]

$$a(t) = \int_{-\infty}^{\infty} d\omega\; a(\omega)\mathrm{e}^{-i(\omega-\omega_0)t} \tag{6}$$

satisfying $[a(t), a^{\dagger}(t')] = \delta(t-t')$ and the constant $\Gamma = (\boldsymbol{\mu}_{eg}\cdot\boldsymbol{\epsilon})^2\mathcal{A}(\bar{\omega})^2$ proportional to the square of the dipole moment.

In addition to the mode defined by the travelling pulse, an atom in free space interacts with an infinitude of other modes that lead to spontaneous emission. We account for this by introducing a coupling to an additional field mode b, leading to the interaction-picture Hamiltonian

$$H_{\rm I}(t) = -\mathrm{i}\hbar\sigma_+\Big(\sqrt{\Gamma}a(t) + \sqrt{\Gamma_\perp}b(t)\Big) + \mathrm{h.c.}, \tag{7}$$

where the new set of white noise operators $b(t)$ satisfying $[b(t), b^{\dagger}(t')] = \delta(t-t')$ represents a collective "environment" mode coupled to the atom. For completeness, we show in Appendix A that this is equivalent to a more realistic model where the environment consists of a discrete set of infinitely many modes.

The interaction Hamiltonian (7) seeks to capture an experimental scenario where only the field in the pulse mode can be measured, while light emitted into the environment is irreversibly lost. Mathematically, this means tracing out the mode b; the resulting reduced dynamics of the atom-pulse subsystem is governed by a master equation in Lindblad form

$$\frac{d\rho(t)}{dt} = -\mathrm{i}\sqrt{\Gamma}\big[\sigma_+ a(t) - \sigma_- a^{\dagger}(t), \rho(t)\big] + \Gamma_\perp\mathcal{D}[\sigma_-]\rho(t), \tag{8}$$

where we have introduced the superoperator $\mathcal{D}[A]\rho = A\rho A^{\dagger} - \frac{1}{2}\big(\rho A^{\dagger}A + A^{\dagger}A\rho\big)$. While a master equation treatment is very useful numerically, for single-photon pulses it will be easier to solve the total unitary dynamics. We take the latter approach in Sec.??.

Note that although the Hamiltonian (7) is obtained in the white noise limit, which is a Markov approximation, this is not enough to have a reduced dynamics in Lindblad form for a generic initial state of the field?? Do you mean the travelling pulse?; however, we have the additional property that the state of the environment is the vacuum and thus temporally uncorrelated. On the contrary, for nonclassical initial states of the field, such as Fock or squeezed states, we have temporal correlations and the reduced dynamics of the atom is non-Markovian [30]. It can generally be described by hierarchies of master equations [23, 31, 32] or by using fictitious cavities [33, 34], as we explain in Sec. II B.

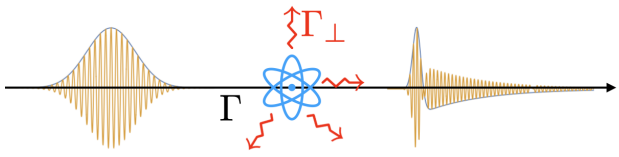

Figure 1. Illustration of the excitation of the atom by a quantum pulse of light (with Gaussian temporal envelope). Γ represents the interaction strength with the pulse mode, while $\Gamma_\perp$ describes emission into other (inaccessible) orthogonal modes. As shown, the shape of the wavepacket is changed by the interaction with the atom. Illustration not to scale.

The interaction Hamiltonian (7) can be used to describe light-matter interactions in different scenarios by assigning different expressions to the coupling constants. In a free-space configuration with the atom probed by paraxial light, there is usually a strong coupling with the environment and a weak coupling with the pulse, resulting in $\Gamma_\perp \gg \Gamma$ [27]. Nonetheless, by matching the pulse spatial and polarization mode to the dipole pattern of the atom, one could in principle obtain a perfect coupling $\Gamma_\perp = 0$ even in free space [9]. However, the scenario $\Gamma_\perp = 0$ is mostly employed to study two-level atoms in one-dimensional waveguides [28, 29].

In this paper, we will not grapple with such model-dependent details and take the Hamiltonian (7) as our starting point until Sec. VI. There we will apply our methods to estimating the dipole moment of the Sodium D?? transition using travelling pulses of quantum light. Furthermore, we will always assume that the atom is initially in the ground state, because we want to model light absorption and the corresponding excitation induced by the pulse. However, if we kept the same Hamiltonian but started the dynamics with the atom in the excited state and both field modes $a(t)$ and $b(t)$ in the vacuum, the overall decay rate would be $\Gamma_{\rm tot} = \Gamma + \Gamma_\perp$ [9, 23, 25, 26], and in free-space this corresponds to the standard rate obtained from Wigner-Weisskopf theory $\Gamma_{\rm tot} = \frac{|\boldsymbol{\mu}_{eg}|^2\omega_0^3}{3\pi\epsilon_0\hbar c^3}$.

2. *Quantum states of the travelling pulse*

A pulse of light travelling in one dimension can be described quantum mechanically using Fock states defined

[1] Formally, the operators $a(t)$ should be treated using quantum stochastic calculus [21, 22]. However, this is uncecessary for our purposes; we refer the reader to some physics-oriented introductions to quantum stochastic calculus in the context of light-matter interaction with pulses of radiation [23–25] .

as [19]

$$|n_\xi\rangle = \frac{1}{\sqrt{n!}}\left(\int d\omega\ \tilde{\xi}(\omega)a^\dagger(\omega)\right)^n|0\rangle, \tag{9}$$

where $\tilde{\xi}(\omega)$ is an arbitrary square-integrable normalised function. As we assume the light to be sufficiently narrowband around the carrier frequency $\bar{\omega}$, we can define the photon-wavepacket annihilation operator

$$A_\xi = \int_{-\infty}^{\infty} dt\ \xi(t)a(t), \tag{10}$$

such that $[A_\xi, A_\xi^\dagger] = 1$ for a spectral amplitude $\xi(\omega)$. The function $\xi(t)$ is the Fourier transform of $\tilde{\xi}(\omega)e^{-\mathrm{i}\bar{\omega}t}$ and represents a temporal wavepacket with modulation at the frequency $\bar{\omega}$, as depicted in Fig. 1.

In this paper we only consider real-valued functions $\xi(t)$, which in frequency domain means $\tilde{\xi}(\omega-\bar{\omega})^* = \tilde{\xi}(\bar{\omega}-\omega)$, e.g. if $\xi(\omega)\in\mathbb{R}$ as often happens, it must be symmetric around the carrier frequency[2]. While we do not consider general situations with arbitrary complex-valued envelopes, our choice covers many practically relevant cases. [@Aiman can you help me with some reference/argument on this?]This is a restricted case. How complicated are the general expressions? For instance, the conclusions of Sec III B, appendix D may not hold for complex pulses. In general $\xi(t)$ can be considered as one element of an orthonormal basis of functions that form a complete set of temporal modes [35–37], e.g. Hermite-Gauss polynomials if $\xi(t)$ is Gaussian. We also assume no detuning between the carrier frequency and the transition frequency of the atom $\bar{\omega} = \omega_0$.

In terms of the photon-wavepacket creation operator $A_\xi^\dagger$, the Fock states (9) can be reexpressed as $|n_\xi\rangle = \frac{1}{\sqrt{n!}}A_\xi^{\dagger n}|0\rangle$. Descriptions of other states such as coherent states

$$|\alpha_\xi\rangle = e^{\alpha A_\xi^\dagger - \alpha^* A_\xi}|0\rangle = e^{-|\alpha|^2/2}\sum_{n=0}^{\infty}\frac{\alpha^n}{\sqrt{n!}}|n_\xi\rangle, \tag{11}$$

with average photon number $\int_{-\infty}^{\infty}dt\langle\alpha_\xi|a^\dagger(t)a(t)|\alpha_\xi\rangle = |\alpha|^2$ and squeezed vacuum states [32, 36]

$$|s_\xi\rangle = e^{\frac{1}{2}\left(sA_\xi^{\dagger\,2} - s^*A_\xi^2\right)}|0\rangle = \frac{1}{\sqrt{\mu}}\sum_{n=0}^{\infty}\left(\frac{\nu}{2\mu}\right)^2\frac{\sqrt{(2n)!}}{n!}|2n_\xi\rangle, \tag{12}$$

where $s = re^{i\phi}$, $\mu = \cosh r$ and $\nu = e^{i\phi}\sinh r$ and the average photon number is $\int_{-\infty}^{\infty}dt\langle s_\xi|a^\dagger(t)a(t)|s_\xi\rangle = \sinh^2 r$ follow.

[2] However an overall global phase, i.e. a purely imaginary $\xi(t)$ corresponding to an antisymmetric $\tilde{\xi}(\omega)$ around the carrier frequency, does not change our analysis.

B. Dynamics of the state in the travelling pulse temporal mode

[Move this to an appendix?] When $\Gamma_\perp = 0$ the Schrödinger equation for the joint pulse-atom system can be formally solved for input pulses containing a finite number of photons, as shown in Ref. [28], but the integrals quickly become intractable as the number of photons increases. However, to the best of our knowledge there is no general approach to obtain the field state analytically for arbitrary Γ and $\Gamma_\perp$. The main difficulty is that the interaction does not only transform the input quantum state, defined in terms the operators $A_\xi^\dagger$, but also changes the temporal mode structure due to the spontaneous emission of the atom, as schematically depicted in Fig. 1.

A more tractable problem is to focus on the output state of the light in a particular temporal mode, i.e. the reduced state obtained by tracing out all the other field temporal modes. In this way, we only take into account the effect that the interaction with the atom has onto the quantum state of the travelling pulse, without taking into account the modifications to the temporal wavepacket due to spontaneous emission.

A powerful formalism to treat this scenario was recently put forward by Kiilerich and Mølmer [33, 34]. Without going into details, the physical system, i.e. the atom interacting with a travelling pulse of radiation, can be mapped to the atom interacting with two fictitious optical cavities u and v, corresponding to the bosonic annihilation operators a_u and a_v, with a time-dependent coupling. The quantum states of the cavity u and v correspond to states of the incoming and outgoing pulse, respectively. The whole dynamics of the composite system can be described by a time-dependent Lindblad equation:

$$\dot{\rho}(t) = -\frac{\mathrm{i}}{\hbar}[H(t),\rho(t)] + \Gamma_\perp\mathcal{D}[\sigma_-]\rho(t) + \mathcal{D}[L(t)]\rho(t), \tag{13}$$

the Hamiltonian reads

$$H(t) = \frac{\mathrm{i}\hbar}{2}\big(\sqrt{\Gamma}g_u(t)a_u^\dagger\sigma_- + \sqrt{\Gamma}g_v^*(t)a_v\sigma_+ + g_u(t)g_v^*(t)a_u^\dagger a_v - \text{h.c.}\big), \tag{14}$$

the time-dependent couplings depend on the shape of the chosen temporal mode as follows

$$g_u(t) = \frac{\xi^*(t)}{\sqrt{1-\int_0^t dt'|\xi(t')|^2}} \quad g_v(t) = -\frac{\xi^*(t)}{\sqrt{\int_0^t dt'|\xi(t')|^2}}, \tag{15}$$

and the collapse operator is

$$L(t) = \sqrt{\Gamma}\sigma_- + g_u(t)a_u + g_v(t)a_v. \tag{16}$$

Crucially, in Eq. (13) excitations can only go from the cavity u to the atom and from the atom to the cavity v [33]. Since we are focusing on the quantum state of the light in the *same* temporal mode as the input pulse, the function $\xi(t)$ appears in both couplings (15), however in

general they could be different. In a spectroscopy setting we can only measure the output light scattered by the two-level atom and thus we will mostly consider the reduced state of the cavity v, i.e. $\rho_v(t) = \mathrm{Tr}_{u,s}\,\rho(t)$.

C. Local quantum estimation theory

Estimation theory quantifies the precision in estimating the true value of a parameter Γ from the experimental observations x distributed according to some probability distribution $p(x|\Gamma)$. Quantum mechanically, $p(x|\Gamma) = \mathrm{Tr}(\rho_\Gamma \Pi_x)$ - the probability distribution of the collected data is obtained from the Born rule. Here ρ_Γ is a mixed quantum state depending on the parameter Γ, Π_x is an element of a positive operator-valued measure (POVM), which mathematically describes a quantum measurement [38], and x labels the possible experimental outcomes. For example, in a photon counting measurement x is the number of detected photons. In this paper, ρ_Γ may correspond either to the joint state of the atom and field or to the reduced state of the field.

If $\tilde{\Gamma}$ is an unbiased estimator of Γ its variance satisfies the Cramér-Rao bound (CRB) [39]

$$\mathrm{Var}[\tilde{\Gamma}] \geq \frac{1}{M\mathcal{C}(\rho_\Gamma, \Pi_x)}, \tag{17}$$

where M is the number of repetitions of the experiment and $\mathcal{C}(\rho_\Gamma, \Pi_x)$ is the classical Fisher information (CFI)[3] defined as

$$\mathcal{C}(\rho_\Gamma, \Pi_x) = \sum_x \frac{1}{p(x|\Gamma)}\left(\frac{\partial p(x|\Gamma)}{\partial \Gamma}\right)^2, \tag{18}$$

where the summation becomes an integral for continuous distributions. Since the inequality (17) can be saturated in the limit $M \to \infty$ [40], e.g., by the maximum likelihood estimator, the CRB encodes the maximal precision that can be extracted by the collecting data from the distribution $p(x|\Gamma)$.

To identify the fundamental quantum limit on the precision of the estimator, the CFI must be maximised over all possible POVMs, obtaining [41–44]

$$\max_{\{\Pi_x\}} \mathcal{C}(\rho_\Gamma, \Pi_x) \leq \mathcal{Q}(\rho_\Gamma), \tag{19}$$

where we introduced the quantum Fisher information (QFI), defined as

$$\mathcal{Q}(\rho_\Gamma) = \mathrm{Tr}\big[\rho_\Gamma L_\Gamma^2\big], \tag{20}$$

where the Hermitian operator L_Γ is called the symmetric logarithmic derivative (SLD) and satisfies the Lyapunov equation

$$2\frac{\partial \rho_\Gamma}{\partial \Gamma} = \rho_\Gamma L_\Gamma + L_\Gamma \rho_\Gamma. \tag{21}$$

The bounds on the estimation precision are thus

$$\mathrm{Var}[\tilde{\Gamma}] \geq \frac{1}{M\mathcal{C}(\rho_\Gamma, \Pi_x)} \geq \frac{1}{M\mathcal{Q}(\rho_\Gamma)}. \tag{22}$$

We assume that M can be made sufficiently large, so that we can safely focus on the CFI and QFI as the relevant figures of merit to quantify the estimation precision. This setting is known as local estimation, since the CFI and QFI are defined locally around the true value of the parameter (ρ_Γ and $\partial_\Gamma \rho_\Gamma$ are evaluated at the true value of Γ in all the equations above). In order to study the problem for small M, non-local approaches such as Bayesian or minimax estimation would be more suitable.

The effect of a generic (nonlinear) reparametrization $\Gamma \mapsto \mu(\Gamma)$ only enters as a multiplicative factor in the CFI and QFI, i.e. $\mathcal{Q}(\rho_\mu) = \mathcal{Q}(\rho_{\Gamma(\mu)})(d\Gamma(\mu)/d\mu)^2$ (and analogously for the CFI). Note that the CFI and QFI are dimensional quantities if the estimated parameter has physical dimensions. Sometimes it is useful to consider the adimensional quantum signal-to-noise ratio (QSNR) $\Gamma^2\mathcal{Q}(\rho_\Gamma)$ that quantifies the relative estimation precision. SNR^2 ??

While the QFI (20) generally does not have a simple closed-form expression and must be evaluated by diagonalizing the density matrix, in some cases more explicit formulas can be obtained. For a pure state $|\Psi_\Gamma\rangle$

$$\mathcal{Q}(|\Psi_\Gamma\rangle) = 4\Big(\langle \partial_\Gamma \Psi_\Gamma | \partial_\Gamma \Psi_\Gamma\rangle - |\langle \partial_\Gamma \Psi_\Gamma | \Psi_\Gamma\rangle|^2\Big). \tag{23}$$

Another case that will be relevant is the rank-2 mixed state $\rho_\Gamma = \big|\tilde{\psi}_e\big\rangle\big\langle\tilde{\psi}_e\big| + \big|\tilde{\psi}_g\big\rangle\big\langle\tilde{\psi}_g\big|$, obtained from tracing out the atomic degrees of freedom from a pure state of the form $|\psi_\Gamma\rangle = |e\rangle|\tilde{\psi}_e\rangle + |g\rangle|\tilde{\psi}_g\rangle$. The two vectors $\big|\tilde{\psi}_e\big\rangle$ and $\big|\tilde{\psi}_g\big\rangle$ capturing the quantum states of the field will neither be normalized nor mutually orthogonal, and generally infinite-dimensional. In this scenario the QFI can be evaluated explicitly without rewriting ρ_Γ on an orthonormal basis, thanks to methods for solving Eq. (21) using non-orthogonal bases [45–47], recently introduced in the context of superresolution imaging. We use this technique in Sec. IV.

Another useful property of the QFI is the extended convexity [48, 49]

$$\mathcal{Q}\left(\sum_m p_{m,\Gamma}\rho_{m,\Gamma}\right) \leq \mathcal{C}(\{p_{m,\Gamma}\}) + \sum_i p_{i,\Gamma}\mathcal{Q}(\rho_{m,\Gamma}), \tag{24}$$

where $\{p_{m,\Gamma}\}$ is a (potentially parameter-dependent) probability distribution and $\{\rho_{m,\Gamma}\}$ are normalized quantum states. In words, this means that the QFI of a generic

[3] Since the CFI depends only on the classical probability distribution we will often use notation $\mathcal{C}(p)$, to indicate the CFI of a particular Γ-dependent distribution p, often dropping the Γ dependence too.

mixture is upper bounded by the CFI of the mixing probability plus the average QFI of the states; this reduces to standard convexity when the mixing probability does not dependent on the parameter. This equation can be understood as a consequence of the monotonicity of the QFI under CPTP maps [50], since the right-hand side of Eq. (24) is the QFI of the state $\sum_m p_{m,\Gamma}\rho_{m,\Gamma}\otimes|m\rangle\langle m|$ while the left-hand side is obtained via its partial trace, potentially losing information. In the context of probabilistic quantum metrology, a state in this form can be obtained by making a selection measurement on an initial state and storing the outcome in an ancillary system that acts as a classical register [51]. If the states $\rho_{m,\Gamma}$ have support in mutually orthogonal subspaces (at least in the neighbourhood of the true parameter value), then the information contained in the classical register $\{|m\rangle\langle m|\}$ is formally redundant, since they are perfectly distinguishable, and Eq. (24) is saturated with equality.

III. SINGLE-PHOTON PULSES

We now begin the presentation of our results on quantum light spectroscopy of a two-level atom using single-photon pulses. This is a simple, yet conceptually beneficial and practically relevant scenario of quantum light spectroscopy. The results of this section can be applied to arbitrary pulse shapes. We present concrete results for a few paradigmatic simple pulse shapes employed in theoretical papers [9], but often focus on a rectangular pulse for the This is more than a mere theoretical exercise as the realization of nontrivial single-photon wavepackets is a well-developed experimental field [52–55].

First, we present the analytical solution available in this case, then we employ it to evaluate the QFI for the case of perfect coupling between the atom and the pulse mode. Finally, we extend the discussion to the case in which the two-level system couples also to the environment, focusing in particular on the free-space case where $\Gamma_\perp \gg \Gamma$ and elaborate on the relation to single-photon absorption spectroscopy.

A. Unitary evolution of atom, pulse and environment

We start with the atom in the ground state. Thus, the global atom-pulse-environment state never contains more than one excitation due to the form of the interaction Hamiltonian (7) This state is given by (omitting the explicit time dependence for brevity)

$$|\Psi\rangle = \psi_e|e\rangle|0_P\rangle|0_E\rangle + |g\rangle(|\psi_{g,P}\rangle|0_E\rangle + |0_P\rangle|\psi_{g,E}\rangle), \tag{25}$$

where $|\psi_{g,P}(t)\rangle = \int_{-\infty}^{\infty} d\tau\psi_{g,P}(t,\tau)a^\dagger(\tau)|0_P\rangle$ and $|\psi_{g,E}(t)\rangle = \int_{-\infty}^{\infty} d\tau\psi_{g,E}(t,\tau)b^\dagger(\tau)|0_E\rangle$ are unnormalized single-photon states in the pulse and environmental modes respectively when the atom is in the ground state. For clarity we have explicitly separated the vacuum in the pulse and environment modes. The scalar function $\psi_e(t)$ is the excitation amplitude of the atom.

Solving the Schrödinger equation $i\hbar\frac{d}{dt}|\Psi(t)\rangle = H_I(t)|\Psi(t)\rangle$ for the interaction-picture Hamiltonian (7) assuming the initial state $|g\rangle\Big(\int_{-\infty}^{\infty} d\tau\xi(\tau)a^\dagger(\tau)|0_P\rangle\Big)|0_E\rangle$ at $t=-\infty$ gives

$$\psi_e(t) = -\sqrt{\Gamma}\int_{-\infty}^{t} dt' e^{-\frac{1}{2}(\Gamma+\Gamma_\perp)(t-t')}\xi(t') \tag{26}$$

$$|\psi_{g,P}(t)\rangle = \int_{-\infty}^{\infty} d\tau\Big(\xi(\tau)+\sqrt{\Gamma}\Theta(t-\tau)\psi_e(\tau)\Big)a^\dagger(\tau)|0_P\rangle \tag{27}$$

$$|\psi_{g,E}(t)\rangle = \sqrt{\Gamma_\perp}\int_{-\infty}^{t} d\tau\psi_e(\tau)b^\dagger(\tau)|0_E\rangle, \tag{28}$$

by following the approach of Ref. [28], see also Ref. [25, Appendix G].[There is a difference wrt [25] at the point $t=\tau$, due to the convention for the value of $\Theta(0)$. Since it is a measure-zero set it should play no role.]Appendix D in published version? Note that for $\xi(t)\in\mathbb{R}$ the evolved wavefunctions remain real. For $\Gamma>0$ there is a nonzero excitation probability $p_e(t)=\psi_e(t)^2$ which tends to zero for large times: $\lim_{t\to\infty}p_e(t)=0$. This happens even when $\Gamma_\perp=0$, meaning that the atom spontaneously emits into the pulse mode; in this case the final state $|\psi_{g,P}^{\infty}\rangle = \lim_{t\to\infty}|\psi_{g,P}(t)\rangle$ is a normalized one-photon wavepacket with amplitude $\xi(\tau)+\sqrt{\Gamma}\psi_e(\tau)$. Note also that the states in Eqs. (25)–(28) are normalized, as we show explicitly in Appendix C.

Assuming the initial spectral/temporal mode of the pulse to be the only one accessible for detection, we trace out both the atom and the environment degrees of freedom, obtaining an incoherent mixture of the vacuum and the modified single photon wavepacket

$$\rho_\Gamma = \big(|\psi_e|^2 + \langle\psi_{g,E}|\psi_{g,E}\rangle\big)|0_P\rangle\langle 0_P| + |\psi_{g,P}\rangle\langle\psi_{g,P}|, \tag{29}$$

where again we have suppressed the explicit time dependence. In the long-time limit $t\to\infty$ the atom decays to the ground state and becomes disentangled with the light, but for $\Gamma_\perp>0$ the initial photon of the pulse is partly lost to the environment.

B. Single-photon QFI: absorption and temporal-mode perturbation

The state (29) has the form $\rho_\Gamma = p_\Gamma|0\rangle\langle 0| + (1-p_\Gamma)|\psi_\Gamma\rangle\langle\psi_\Gamma|$, where we have now highlighted the dependence on the parameter Γ and written it in terms of a normalized single-photon state $\langle\psi_\Gamma|\psi_\Gamma\rangle=1$. It would be useful to express p_Γ and $|\Psi_\Gamma\rangle$ in terms of the quantities in Eq. 29 here. Since we are dealing with real-valued wavefunctions, $\langle\partial_\Gamma\psi_\Gamma|\psi_\Gamma\rangle=0$ and the QFI of ρ_Γ is simply the QFI of the two-outcome probability distribution

$\{p_\Gamma, 1-p_\Gamma\}$ plus the QFI of the pure single-photon state multiplied by the corresponding probability:

$$\mathcal{Q}(\rho_\Gamma) = \frac{(\partial_\Gamma p_\Gamma)^2}{p_\Gamma(1-p_\Gamma)} + (1-p_\Gamma)4\langle\partial_\Gamma\psi_\Gamma|\partial_\Gamma\psi_\Gamma\rangle \tag{30}$$

$$= \mathcal{C}(p_\Gamma) + \tilde{\mathcal{Q}}(|\psi_\Gamma\rangle). \tag{31}$$

This form corresponds to the right-hand side of (24) as expected, since the two pure states in the mixture are orthogonal and the vacuum contains no information on Γ. Note the two contributions to the fundamental limit of estimating Γ: (i) the probability p_Γ of losing a photon from the pulse mode giving the CFI $\mathcal{C}(p_\Gamma) = \frac{(\partial_\Gamma p_\Gamma)^2}{p_\Gamma(1-p_\Gamma)}$, which we call the absorption contribution to the total QFI $\mathcal{Q}(\rho_\Gamma)$, and (ii) the perturbation to the temporal shape of the single-photon wavepacket gives the QFI of the pure state single-photon wavepacket (rescaled by the corresponding probability of not losing a photon) $\tilde{\mathcal{Q}}(|\psi_\Gamma\rangle) = (1-p_\Gamma)4\langle\partial_\Gamma\psi_\Gamma|\partial_\Gamma\psi_\Gamma\rangle$, which we call the temporal-mode perturbation contribution. In Appendix D we report more explicit expressions, using an alternative formulation, written in terms of the unnormalized single photon state, which is more convenient for evaluation.

Is (i) available in classical spectroscopy and (ii) only in quantum spectroscopy?

We next discuss the means of attaining (i) and (ii) respectively.

For any real wavefunction $\psi(\tau)$ with real derivative $\partial_\Gamma\psi(\tau)$, the CFI of the probability distribution $\psi(\tau)^2$ saturates the QFI, since $\int d\tau\left[\partial_\Gamma\psi(\tau)^2\right]^2/\psi(\tau)^2 = 4\int d\tau[\partial_\Gamma\psi(\tau)]^2$. In the long time limit $t\to\infty$ this is the standard "direct measurement" of the photon arrival time, optimal for estimating the fluorescence lifetime [11]. [This requires some assumptions on the detectors though. I do not know in which situations it is practically feasible.] We remark that in lifetime estimation problems, one usually considers a simplified picture in which the atom is initially excited and the excitation process itself is not modeled, unlike in this work. However, in general the state ρ_Γ contains less than one photon on average and the QFI (31) is saturated when it is possible to distinguish the vacuum from the single-photon component. In other words, the first absorption contribution in (31) is obtained by measuring the photon loss, similarly to absorption spectroscopy, while the second temporal-mode perturbation contribution is obtained by measuring the arrival time of the surviving photon. Confused by this para. Is this about attaining (i) only, and the next para about (ii)?

One possibility is to only measure the original, unperturbed, temporal mode of the pulse. In the spirit of Sec. II B, we seek to measure changes in the quantum state of the original incident pulse after interacting with the atom. For single photons, this corresponds to a two-outcome POVM with elements $\Pi_1 = |\xi\rangle\langle\xi|$ and $\Pi_0 = \mathbb{1} - \Pi_1$, where $|\xi\rangle = \int_{-\infty}^{\infty} d\tau\xi(\tau)a^\dagger(\tau)|0_P\rangle$ is the initial state of the single-photon pulse. The probability

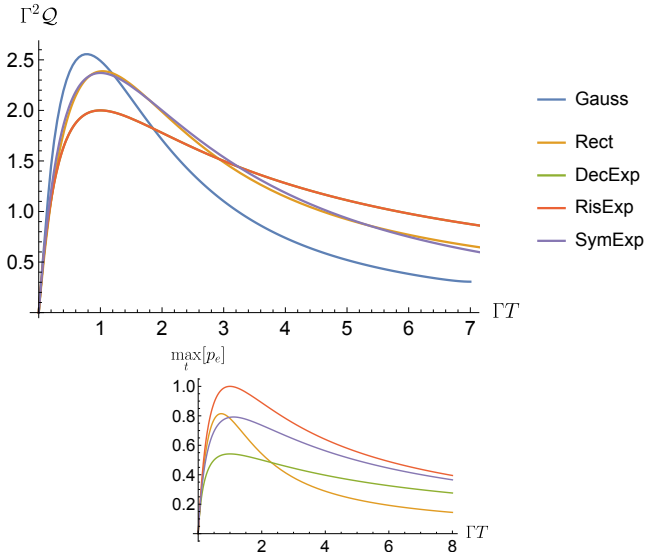

Figure 2. Plot of the quantum signal-to-noise-ratio $\Gamma^2\mathcal{Q}(\rho_\Gamma^\infty)$ about the atom-pulse coupling parameter Γ for the asymptotic single-photon wavepacket (perfect coupling $\Gamma_\perp = 0$), as a function of ΓT. The pulse duration T is defined as the standard deviation of the original photon wavepacket. The pulse shapes are (from top to bottom in the legend): Gaussian, rectangular, decaying, rising and symmetric exponential (overlapping in the plot). Inset [will become an inset when we agree on the plots]: plot of the maximal excitation probability of the two-level atom, for the same pulse shapes (except the Gaussian Why not?).

of seeing such a detector click for the state (29) is thus $p_{\rm orig} = \mathrm{Tr}[\Pi_1\rho_\Gamma(t)] = |\langle\xi|\psi_{g,P}(t)\rangle|^2$. The performance of this measurement in attaining the quantum limit (31) is addressed in the next section.

Another possibility is to detect the emitted light in different temporal modes. For a single photon pulse, this corresponds ideally to a rank-1 projective POVM $|\xi_k\rangle\langle\xi_k|$ on an orthonormal basis of temporal modes $|\xi_k\rangle = \int_{-\infty}^{\infty} d\tau\xi_k(\tau)a^\dagger(\tau)|0_P\rangle$. Cite Aiman's paper which does this.

[Another possibly interesting case is a projection onto output state $\psi_{g,P}$, which also saturates the QFI (at least, I've checked this for $\Gamma_\perp = 0$ and $t\to\infty$). This is often an optimal measurement in local quantum metrology, where a small discrepancy from a probability of 1 carries a lot of information about the small deviation from the true parameter value, but I think it is not really feasible in general, so I would not mention it] Why not?

C. Perfect atom-pulse coupling

To clarify our understanding of quantum light spectroscopy using single photon pulses, we now focus on perfect atom-pulse coupling by setting $\Gamma_\perp = 0$.

1. Long-time results

We start by studying the asymptotic case $t \to \infty$, when the final state of the pulse contains exactly one photon, and is pure and disentangled from the atom. Then all the information about the parameter Γ is encoded in the temporal shape of the wavepacket, which is perturbed due to the interaction. Do you mean $p_\Gamma = 0$? If yes, say so. Is this true for all pulses? The table in the Appendix E shows that $p_e(\infty) \neq 0$ for the rect. pulse. In Fig. 2 we show the asymptotic QSNR $\Gamma^2 \mathcal{Q}(\rho_\Gamma^\infty)$ as a function of the pulse duration, for various pulse shapes. The mathematical descriptions of the pulse shapes considered in Fig. 2 are provided in Appendix E, together with the available analytical expressions for the quantities of interest [4]. Note that by employing the adimensional QSNR the the parameters enter only in the combination ΓT. How do you know this is true for arbitrary pulses?

The various pulse shapes display the same qualitative behaviour: The QSNR increases linearly as the pulse duration increases from $\Gamma T = 0$. There is a limited dependence on the particular shape. It reaches a maximum for a value around the fluorescence time $\Gamma T = 1$. Overall, there is a mild dependence on the particular shape. This behaviour is similar to that of the maximum excitation probability of the atom [9, 56], shown in the inset of Fig. 2. One might naively think that an higher excitation probability of the atom, which corresponds in some sense to a "better" interaction between the atom and the pulse, would correspond to a higher QFI of the outgoing pulse of light. Our results show otherwise. Firstly, the optimal pulse duration for a given pulse shape for the two tasks are different. Secondly, while a rising and a decaying exponential pulse of the same duration yield the same asymptotic QFI, i.e., overlapping curves in Fig. 2, the rising exponential is optimal to excite the atom [56] (reaching one in the inset plot), while the decaying exponential performs much worse.

In Fig. 3, we show how much information can be extracted by detecting the photon in the original temporal wavepacket compared to the information available in the asymptotic state by plotting the ratio between the CFI of this detection strategy $\mathcal{C}(p_{\text{orig}})$ (for $t \to \infty$) and the asymptotic QFI (already plotted on its own in Fig. 2). In the limit of short pulses $T \to 0$ this ratio tends to the value $1/2$; curiously it is always $1/2$ for the rising and decaying exponentials. This has been proven exactly for all pulse shapes except for Gaussian pulses, for which all the quantities must be evaluated by solving the integrals

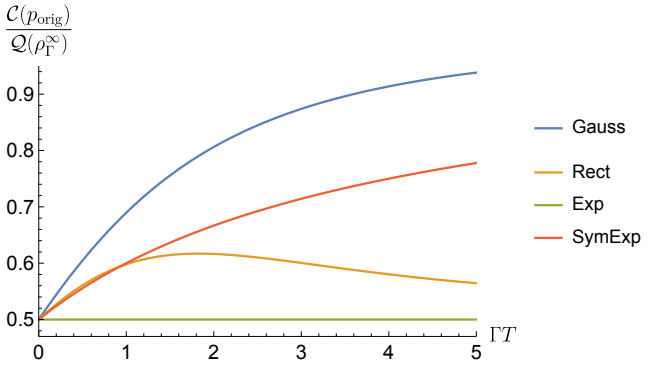

Figure 3. Plot of the ratio between the FI $\mathcal{C}(p_{\text{orig}})$ for photodetection in the original pulse mode and the asymptotic QFI, for different pulse shapes (the legend "Exp" stands for both rising and decaying exponential shape).

numerically. We conjecture this to be a general feature of this metrological problem in the $T \to 0$ limit, since the details of the pulse shape should be less relevant in this regime.

It is remarkable that for quantum light spectroscopy with single-photon pulses, this simple detection strategy yields a substantial fraction of the maximal information available, quantified by the asymptotic QFI, about the parameter. As we show in the next section, measuring the photon in the original temporal mode has the advantage that the information can be obtained rather rapidly after the interaction (about femto- or picoseconds for ultrafast pulses), without the need to wait for the atom to decay (timescale of nanoseconds in standard atomic and molecular systems). While this may be of limited appeal in spectroscopy, it may be exploited in quantum information processing.

Finally, one could in principle, optimize the pulse shape to maximise the QSNR. Given the recent advances in the experimental shaping of single-photon wavepackets,e.g. [52–55], this could be a practically interesting question.

2. Finite-time results

For finite t, the atom remains partially excited and the overall atom-field state entangled, so the absorption contribution $\mathcal{C}(p_\Gamma)$ in (31) now plays a role [5]. To highlight the qualitative features in this case, we focus on a rectangular pulse $\xi(t) = \sqrt{1/T}\Theta(t)\Theta(T-t)$ supported on an

[4] There is no unique way to define the duration of a pulse, since most pulses are supported on an open interval. In order to make a meaningful comparison, the definition of "pulse duration" used in in Fig. 2 is the standard deviation of the single-photon probability distribution $|\xi(\tau)|^2$ in absence of interaction. While this makes the comparison more meaningful, it does not always correspond to the intuitive notion of pulse duration when the support is finite, e.g. for a rectangular pulse.

[5] For real-valued $\xi(t)$ that we consider, no additional information would be available by having access to the global field-atom pure state. In fact, there is no information encoded in the relative phase of the state $\psi_e|e\rangle|0_P\rangle + |g\rangle|\psi_{g,P}\rangle$ and it is easy to see that its QFI is equal to the QFI [Do you mean the second term in (31)?] of the pulse state (29) with $\Gamma_\perp = 0$, i.e. $|\psi_e|^2|0_P\rangle\langle 0_P| + |\psi_{g,P}\rangle\langle\psi_{g,P}|$.

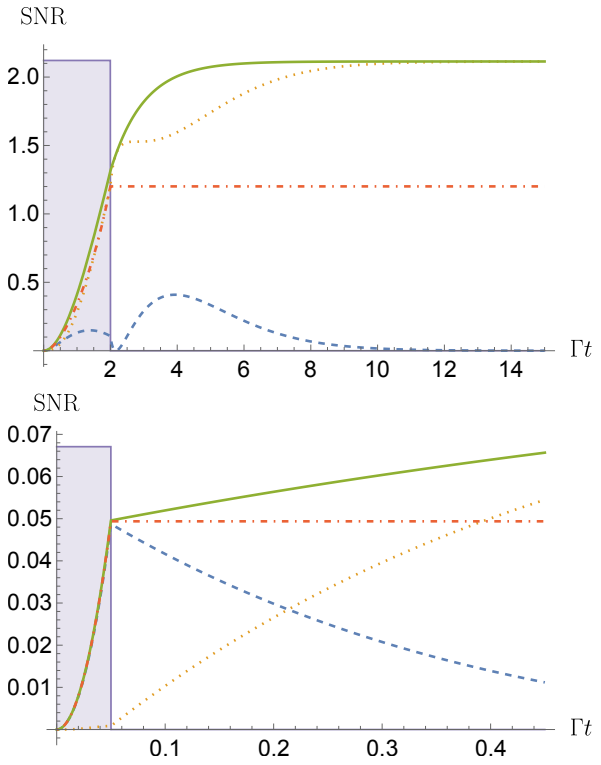

Figure 4. Plot of the classical and quantum SNR for the parameter Γ, for a rectangular single-photon pulse, with $\Gamma_\perp = 0$. Top: $\Gamma T = 2$,bottom: $\Gamma T = 1/20$. The dashed lines represent the absorption component $\Gamma^2\mathcal{C}(p_\Gamma)$, the dotted lines represent the pure state contribution $\Gamma^2\tilde{\mathcal{Q}}(|\psi_\Gamma\rangle)$ and the full lines represent the full QSNR $\Gamma^2\mathcal{Q}(\rho_\Gamma)$ (the sum of both terms). The dot-dashed lines represent the SNR $\Gamma^2\mathcal{C}(p_{\rm orig})$ for photodetection in the original temporal mode. The shaded region shows the pulse shape as a guide for the eye (not in scale on the vertical axis). The dotted lines are hard to see. Also in Fig. 5.

interval of duration T[6], starting at $t_0 = 0$, where $\Theta(x)$ is the Heaviside step function. This choice makes both analytical calculations cleaner (see first row, last two columns in Table. .. in Appendix ...) and the identification of the beginning and the end of the pulse unambiguous.

In Fig. 4 we plot the two contributions to the QFI (31) separately as a function of time, as well as the CFI $\mathcal{C}(p_{\rm orig})$ obtained by detecting the photon in the original temporal mode. For a pulse of duration comparable to the fluorescence lifetime, $\Gamma T = 2$, the upper panel shows that the total QFI approaches its asymptotic value by an interplay of the two contributions and for large times only the temporal-mode perturbation is relevant, as expected from the preceding long-time analysis. The dot-dashed line represents the information obtained by detecting the

[6] For a rectangular pulse, T is unambiguously the "pulse duration", yet in Fig. (2), for comparison purposes, the pulse duration was chosen instead as the standard deviation $T/\sqrt{12}$ of the corresponding uniform distribution.

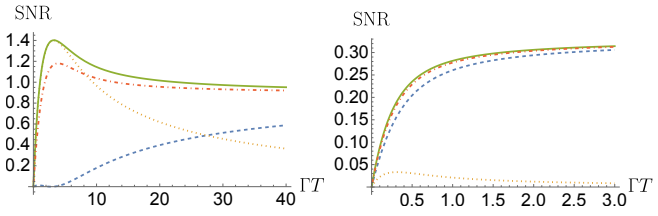

Figure 5. Plot of the classical and quantum SNR. Absorption contribution $\Gamma^2\mathcal{C}(p_\Gamma)$ (dashed blue), temporal-shape perturbation contribution $\Gamma^2\tilde{\mathcal{Q}}(|\psi_{g,P}\rangle)$, whole QSNR $\Gamma^2\mathcal{Q}(\rho_\Gamma^\infty)$ (solid green, sum of the previous two) and SNR $\Gamma^2\mathcal{C}(p_{\rm orig})$ for the original temporal mode (dot-dashed red). Left: $\Gamma_\perp = \Gamma/2$; right: $\Gamma_\perp = 10\Gamma$. Also make upper/lower like Fig. 4 for consistency.

photon wavepacket in its initial temporal mode, and it settles to a value around half seems more than 1/2?? of the asymptotic QFI, as previously shown in Fig. (3). After the pulse has finished interacting with the atom, this information remains constant although the atom continues to emit spontaneously. [[This spontaneous emission is into the mode we are measuring, so why is this constant?]] The qualitative behaviour in this figure will be exhibited by other pulse shapes that are well-localised.

The lower panel of Fig. 4 presents the results for a much shorter pulse, $\Gamma T = 1/20$. In this case the photon interacts with the atom for a short time and there is only a small distortion to the photon wavepacket. This is witnessed by the fact that the dotted line representing the temporal-mode perturbation contribution $\tilde{\mathcal{Q}}(|\Psi_\Gamma\rangle)$ increases only slightly while the pulse is interacting with the atom (shaded region). On the other hand, during the interaction most of the information is obtained by measuring the absorption probability p_Γ, which in this regime practically coincides with $p_{\rm orig}$ and we have $\mathcal{C}(p_\Gamma) \approx \mathcal{C}(p_{\rm orig})$ in this region of the plot. However, after the interaction is over $\mathcal{C}(p_{\rm orig})$ remains unchanged, exactly as in the upper panel, while $\mathcal{C}(p_\Gamma)$ decreases and $\tilde{\mathcal{Q}}(|\Psi_\Gamma\rangle)$ increases as the atom decays back to the ground state.

D. Free-space scenario

We now deal with a nonzero coupling to the additional environmental field modes, i.e., $\Gamma_\perp > 0$. For simplicity, we focus on asymptotic results and present results for a rectangular pulse; qualitatively similar results can be obtained for other shapes. In Fig. 5 we show two exemplary cases, one (left panel) where $\Gamma_\perp$ is smaller but comparable to Γ, $\Gamma_\perp = \Gamma/2$ and one (right panel) where the coupling to the environment is significantly more relevant $\Gamma_\perp = 10\Gamma$. For larger $\Gamma_\perp$ the temporal-mode perturbation contribution is less important and almost all the information can be retrieved by restricting measurements to the incoming temporal mode. [[The SNR is less than 1. This is for $M = 1$. Scales as $\sqrt{M}$?]]

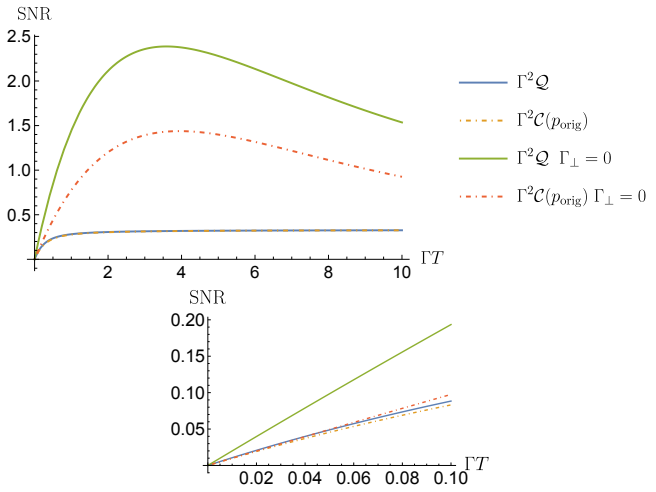

Figure 6. Plot of the QSNR (solid lines) and of the classical SNR $\Gamma^2\mathcal{C}(p_{\rm orig})$ (dot-dashed lines) for $\Gamma_B = 10\Gamma$ (two lower curves) and for perfect coupling $\Gamma_B = 0$ (two top curves). Inset: zoom on the region close to $\Gamma T = 0$.Γ_B??

The parameter choice $\Gamma_\perp/\Gamma = 10$ is intended to capture a pulse interacting with an atom in free space, without particular geometries to enhance the coupling. It is comparable to that for the Na D?? transition we consider in Sec. VI. In general, for $\Gamma_\perp \gg \Gamma$ the atom is coupled more strongly with the vacuum environment than with the pulse and after the excitation will predominantly spontaneously emit into the environmental modes.

In Fig. 6 we compare the total QFI (including both contributions from (31)) and the CFI of the original temporal mode for $\Gamma_\perp/\Gamma = 10$ with that for the perfect-coupling case $\Gamma_\perp = 0$ considered in the previous section. As expected, a larger $\Gamma_\perp$ decreases both the QFI and the CFI. However, in the region of short pulses (shown in the inset), the CFI $\mathcal{C}(p_{\rm orig})$ of the perfect coupling case follows closely the CFI and the QFI of the curves for $\Gamma_\perp = 10\Gamma$. This observation is confirmed more generally. Indeed using the analytical expressions in Table ... of Appendix ... we can show that

$$\lim_{\Gamma_\perp\to\infty}\lim_{T\to 0}\frac{\mathcal{Q}(\rho_\Gamma(\Gamma_\perp),T)}{\mathcal{C}(p_{\rm orig}(\Gamma_\perp=0,T))} = 1, \tag{32}$$

where we have highlighted the dependence on the parameters $\Gamma_\perp$ and T. [I've struggled a lot with the notation, suggestions are welcome.] Notice that formally these limits cannot be exchanged, since $\lim_{\Gamma_\perp\to\infty}\mathcal{Q}(\rho_\Gamma(\Gamma_\perp)) = 0$.

Physically, the above observation means the following: The information obtained during the interaction between the atom and the pulse is the same regardless of the presence of additional environment modes because the pulse is so short[7] that the spontaneous emission terms can be neglected during this part of the dynamics. Moreover, in this limit all the information on Γ is entirely retrieved by considering only the original temporal mode; this motivates the next section on more general quantum states. However, by waiting until the atom decays by spontaneous emission, additional information can be obtained if the emitted photon can be measured ($\Gamma_\perp = 0$ case) but nothing more if it decays into inaccessible modes ($\Gamma_\perp \gg \Gamma$).

[7] For $\Gamma_\perp > 0$ a pulse as "short" if it interacts with the atom much faster than the overall lifetime of the atom, i.e., $T(\Gamma_\perp + \Gamma) = T\Gamma_{\rm tot} \ll 1$.

IV. SHORT PULSES IN ARBITRARY STATES

[[Arbitrary: This is still 'single-mode' as ξ is a function of a single variable. Or does this apply to $\xi(\omega_1, ..., \omega_l)$ that can include entangled states etc.?]]

For short times $t \ll 1/(\Gamma_\perp + \Gamma)$ the spontaneous emission of the atom, either back into the pulse mode or into environmental modes orthogonal to the pulse mode can be neglected. In that regime, for short pulses $\xi(t)$ with $T \ll 1/(\Gamma_\perp + \Gamma)$, the evolution of the atom-field state evolved according to the master-equation (8) can be approximated by a unitary evolution obtained from time-dependent Jaynes-Cummings (JC) interaction between the pulse temporal mode and the atom

$$H_{\rm JC}(t) = \mathrm{i}\hbar\sqrt{\Gamma}\xi(t)\Big(A_\xi\sigma_+ - A_\xi^\dagger\sigma_-\Big). \tag{33}$$

In this limit the interaction with the two-level atom does not modify the pulse temporal mode, but only affects the quantum state of the field in this mode. The time-dependence of the Hamiltonian is trivial and the solution is the same as in the standard cavity-based JC model with the substitution $t \mapsto \int_0^t \xi(t')dt' = G_t$.?? For an initial state $|\psi_0\rangle = \sum_k^\infty \psi_k|k_\xi\rangle|g\rangle$, where $|n_\xi\rangle$ $|k\rangle$?? are the Fock states (9) in the pulse mode, the evolved state is [57]

$$\begin{aligned}|\psi(t)\rangle =& -i\sum_{n=0}^{\infty}\sin\Big(\sqrt{\Gamma}G_t\sqrt{n+1}\Big)\psi_{n+1}|e,n_\xi\rangle + \\ &+\sum_{n=0}^{\infty}\cos\Big(\sqrt{\Gamma}G_t\sqrt{n}\Big)\psi_n|g,n_\xi\rangle \\ =&|e\rangle\Big|\tilde\psi_e(t)\Big\rangle + |g\rangle\Big|\tilde\psi_g(t)\Big\rangle,\end{aligned} \tag{34}$$

where we have introduced two unnormalized field states for later convenience.

We have numerically checked the validity of this approximate model by employing the methods of Sec. II B, as well as a different method based on the decomposition into a truncated basis of orthonormal temporal modes [58]. This approximation is also consistent with the fact that for intense classical? pulses of light interacting with a two-level atom, Rabi oscillations can be observed in with?? the pulse temporal mode [23, 24, 27]. Finally, the method of Sec. II B can be reformulated in a way that resembles the JC interaction (33) for any pulse duration, at the cost of including an additional interaction between the system

and an extra orthogonal mode [59]. Indeed, we have also checked numerically that in this reformulation the additional orthogonal mode remains essentially unpopulated in the regime of validity of our approximation.

The main advantage of making this approximation is that we can directly apply existing results regarding the estimation of the coupling constant of the JC model [60]. Firstly, the overall atom-field QFI is proportional to the variance of the generator of the unitary calculated over the initial state and the time-dependent details of the problem enter only as a multiplicative factor:

$$\mathcal{Q}(|\Psi_{AF}(t)\rangle) = 4\frac{G_t^2}{\Gamma}\mathrm{Var}_{|\Psi_{AF}(0)\rangle}\left[A_\xi\sigma_+ - A_\xi^\dagger\sigma_-\right]. \quad (35)$$

For an arbitrary pulse shape, its duration can be factored out as $\xi(t) = \frac{1}{\sqrt{T}}f\left(\frac{t-t_0}{T}\right)$, where $f(x)$ is the scale-invariant shape function [25], dimensionless and squared-normalized $\int dx f(x)^2 = 1$. A change of variable gives $G_t = \sqrt{T}\int_{-t_0/T}^{(t+t_0)/T} dx f(x)$. This means that within this approximation the global atom-field QFI $\mathcal{Q}(|\Psi_{AF}\rangle)$ is linear in the pulse duration T, and different shapes only induce different proportionality constants.

Secondly, for an atom initially in the ground state and any Fock state wavepacket $|n_\xi\rangle$, the QFI of the reduced field state after the interaction is equal to the pure-state QFI $\mathcal{Q}(|\Psi_{AF}\rangle)$ of the composite field-atom system [60]. The same holds also for the reduced atomic state. This is practically irrelevant as the atom cannot be measured directly. Moreover, the reduced state of the field is always diagonal in the Fock basis and photon counting is thus the optimal measurement that attains the QFI.

In other words, for Fock-state wavepackets no information is lost due to the impossibility of measuring the atom. Counting the photons in the original pulse temporal-mode after the interaction is optimal, at least in the regime of validity of the JC approximation. This resembles an analogous result in absorption spectroscopy using single-photon states [10] (formally equivalent to loss estimation [61]), where even being able to measure lost photons would yield no additional information about the absorption (loss) rate [18]. The analogy between the two problems goes further, since for both Γ estimation (in the approximate JC regime) and bosonic loss estimation, the QFI of a Fock probe state is proportional to the number of photons. Thus, the fundamental quantum limit set by n single-photon states or a single n-photon state are identical.

For other states of the field, however, we need to take the partial trace over the atomic system, leading us to the rank-2 field state

$$\begin{aligned}\rho_F(t) &= \left|\tilde{\psi}_e(t)\right\rangle\left\langle\tilde{\psi}_e(t)\right| + \left|\tilde{\psi}_g(t)\right\rangle\left\langle\tilde{\psi}_g(t)\right| \\ &= p_e(t)|\psi_e(t)\rangle\langle\psi_e(t)| + p_g(t)|\psi_g(t)\rangle\langle\psi_g(t)|,\end{aligned} \quad (36)$$

for which can employ the formulas Eqn.numbers ??mentioned in Sec. II and reported in Appendix B.

The approximate hamiltonian (33) will be applied to estimating the dipole moment of the Na D?? transition in Sec. VI.

V. ENTANGLED BIPHOTON PROBES

[[Add a simple diagram of the setup.]]

We consider a so-called linear biphoton setup as in Fig. **??** in which only one of the two spatially distinct modes of an initial entangled biphoton state interacts with the atom, i.e. the signal, while the other mode acts as the idler. This is the simplest instance of entangled light for spectroscopy - the archetypal instance of quantum light spectroscopy [1, 3, 62]. Similar setups have already been employed to show some form of quantum advantage in experiments [@Aiman: please add the relevant references]. [[Experiments or proposed experiments?]] Our objective is to quantify the performance of entangled states in the simple spectroscopic setup of Fig. **??**.

Theoretically, the statistics generated by a setup relying only on coincidence measurements can be reproduced exactly without the need of entanglement, as pointed out by Stefanov [16]. Moreover, as only one of the entangled photons interacts with the sample in Fig. **??**, the setup is formally equivalent to the use of noiseless ancillas in quantum metrology. Therein, it is well-known that entanglement with ancillas is not advantageous in the case of noiseless unitary dynamics, but may can be useful in presence of noise [63]. The exact conditions when noiseless ancillas are advantageous in quantum metrology remain unknown [64].

We limit ourselves to the case of perfect coupling ($\Gamma_\perp = 0$), but stress that in the short pulse limit spontaneous emission may be neglected. Thus a nonzero coupling with additional environment modes would not change the results. [[What is the definition of pulse width? Because of time-freq. entanglement, there is none?]] As the biphoton pulse becomes entangled with the atom, the dynamics of the field is not unitary and the initial entanglement between the signal and idler modes could be useful.

In this Section, we show this to be untrue for estimating the coupling parameter Γ, under some assumptions on the joint spectral amplitude that include those commonly generated by parametric down-conversion (PDC). Different conclusions are reached for the estimation of different atomic parameters. These will be presented in forthcoming works [65, 66].

The biphoton states obtained from a low-gain PDC process is given by

$$|11_{\mathrm{ent}}\rangle = \int d\omega_\mathrm{s} d\omega_\mathrm{i} \tilde{\Phi}(\omega_\mathrm{s},\omega_\mathrm{i}) a_\mathrm{s}^\dagger(\omega_\mathrm{s}) a_\mathrm{i}^\dagger(\omega_\mathrm{i})|00\rangle, \quad (37)$$

where $\tilde{\Phi}(\omega_\mathrm{i},\omega_\mathrm{s})$ is the joint spectral amplitude (JSA) depends on the envelope of the pump field and the phase-matching function [67] $\omega_\mathrm{s},\omega_\mathrm{i}$ denote the signal an idler frequencies respectively.

For the moment, we do not specify a particular form, but in the next section we will consider a realistic Gaussian spectral density.

The JSA admits a Schmidt decomposition in terms of

discrete Schmidt modes:

$$|11_{\rm ent}\rangle = \sum_k r_k \hat{A}_k^\dagger \hat{B}_k^\dagger |00\rangle = \sum_k r_k |\xi_k\rangle|\phi_k\rangle, \tag{38}$$

where $\hat{A}_k^\dagger$ and $\hat{B}_k^\dagger$ are bosonic creation operators for each Schmidt mode of the signal and idler modes respectively, $|\xi_k\rangle$, $|\phi_k\rangle$ are the respective single-photon wavepackets and r_k are positive Schmidt weights [68, 69]. For instance, a Gaussian JSA has Hermite-Gauss functions as Schmidt modes [70].

As we have done so far, we assume that the carrier frequency $\bar{\omega}_{\rm s}$ of the signal photon [[How do we define the frequency of one half of the entangled state?]] is equal to the transition frequency of the two-level atom and that the joint spectral density is sufficiently narrow-band around the central carrier frequencies $\bar{\omega}_{\rm s}$ and $\bar{\omega}_{\rm i}$. In analogy with the single-photon case, we assume the time-domain envelope $\Phi(t_{\rm i}, t_{\rm s})$, i.e. the Fourier transform of $\tilde{\Phi}(\omega_{\rm i}, \omega_{\rm s})e^{-{\rm i}(\bar{\omega}_{\rm i} t_{\rm i} + \bar{\omega}_{\rm s} t_{\rm s})}$, to be real-valued so that we can choose the time-envelopes of the signal photon Schmidt modes $\xi_k(t)$ to be real valued as well (additional global phase factors that may arise from the decomposition can be included in the definition of the idler photon modes). We can thus take the same approximations explained in Sec. II and consider and interaction-picture Hamiltonian identical to (5) with the substitution $a(t) \mapsto a_{\rm s}(t) \otimes \mathbb{1}_i$, i.e. only the signal mode interacts with the atom. By linearity we can thus employ the previous single-photon solution given by Eqs. (25), (26) and (27) (here for $\Gamma_\perp = 0$) and apply it to the wavepackets $\xi_k(t)$ of the signal mode:

$$\begin{aligned} U(t) \otimes \mathbb{1}_{\rm i} |g\rangle|11_{\rm ent}\rangle &= \sum_k r_k (U(t)|g\rangle|\xi_k\rangle)|\phi_k\rangle \\ &= \sum_k r_k (\psi_{e,k}(t)|e\rangle|0\rangle_s + |g\rangle|\psi_{g,k}(t)\rangle)|\phi_k\rangle. \end{aligned} \tag{39}$$

Since the idler photons modes are orthogonal, i.e. $\langle\phi_j|\phi_k\rangle = \delta_{jk}$ and all the amplitudes $\psi_{e,k}(t)$, $\psi_{g,k}(t,\tau)$ are real we have the following chain of equalities:

$$\begin{aligned} \mathcal{Q}_\Gamma(|11_{\rm ent}(t)\rangle) &= \sum_k r_k^2 \mathcal{Q}(\psi_{e,k}(t)|e\rangle|0\rangle + |g\rangle|\psi_{g,k}(t)\rangle) \\ &= \sum_k r_k^2 \mathcal{Q}\big(\psi_{e,k}(t)^2|0\rangle\langle 0| + |\psi_{g,k}(t)\rangle\langle\psi_{g,k}(t)|\big) \\ &= \mathcal{Q}\left(\sum_k r_k^2 \left[\psi_{e,k}(t)^2|0\rangle\langle 0| + |\psi_{g,k}(t)\rangle\langle\psi_{g,k}(t)|\right] \otimes |\phi_k\rangle\langle\phi_k|\right). \end{aligned} \tag{40}$$

The first equality means that no information on the parameter is stored in the coherences between different Schmidt modes and thus the idler modes act only as a classical register for the labels k. The second equality is the same observation we have made previously: for single-photon wavepackets $\xi_k(t) \in \mathbb{R}$ the whole atom-field information on Γ is fully contained in the field reduced state and the partial trace over the atom subsystem preserves the QFI. In the third equality, we have simply stressed that this corresponds to the QFI of an initial classically correlated state $\sum_k r_k^2 |\xi_k\rangle\langle\xi_k| \otimes |\phi_k\rangle\langle\phi_k|$ instead of an entangled state. This is equivalent to probing the atom with randomly chosen single photon states $|\xi_k\rangle$ with probability r_k^2, but retaining the knowledge on each value k, e.g. detecting the idler photons in the Schmidt modes to perform heralded state preparation of single-photon wavepackets of the signal mode. If the knowledge on the values k is not available one is left with the mixed single-photon state $\sum_k r_k^2 |\xi_k\rangle\langle\xi_k|$ obtained by tracing out the idler mode. Such a spectrally mixed single-photon state yields in general less information on Γ as shown by the convexity property of the QFI (24). This is true also in the asymptotic limit $t \to \infty$: even if the final states in the mixture are pure and orthogonal $\langle\psi_{g,k}^\infty|\psi_{g,j}^\infty\rangle = \delta_{jk}$, they do not remain orthogonal by changing slightly the parameter value, i.e. $\langle\psi_{g,k}^\infty|\partial_\Gamma\psi_{g,j}^\infty\rangle \neq 0$.

Since the QFI (40) is a convex sum of the QFI of the different Schmidt-modes we immediately see that in principle it is always better to prepare deterministically the single-photon wavepacket in the mode ξ_k with the largest QFI $\max_k \mathcal{Q}(|\psi_{e,k}(t)|^2|0\rangle\langle 0| + |\psi_{g,k}(t)\rangle\langle\psi_{g,k}(t)|)$. This clearly shows that entanglement is not a fundamental resource, since there is always a single-photon wavepacket that gives better precision. However, we note that it could be easier or more practical to implement entangled-state strategies rather than some theoretically superior non-entangled one. To make things more concrete, in the next section we show that for a realistic Gaussian joint spectral density coming from PDC, the additional entanglement actually decreases the overall QFI and it is always better to employ a Gaussian single-photon wavepacket.

VI. DIPOLE MOMENT ESTIMATION OF A SODIUM ATOM IN FREE SPACE

We consider again the physical light-matter interaction Hamiltonian originally introduced in Sec. II, since here we rephrase estimation of Γ to the more physical problem of estimating the dipole-moment $\mu = \boldsymbol{\mu}_{eg} \cdot \boldsymbol{\epsilon}$ (we further assume the polarization vector is directed in the same direction as the dipole-moment vector). This parameter is related to the pulse coupling rate we have considered so far as $\Gamma = \mu^2 \mathcal{A}(\bar{\omega})^2$, where we assume that the constant $\mathcal{A}(\bar{\omega}) = \sqrt{\bar{\omega}/(4\pi\hbar\epsilon_0 c A)}$ of the propagating field is known, so that estimating Γ or μ are formally equivalent problems.

To obtain concrete numbers, we use the experimental data reported in Ref. [71] for the D_2 transition of a sodium atom. Specifically, we set the dipole moment $\mu = 2.988 \cdot 10^{-29}{\rm C} \cdot m = 1.868 \cdot 10^{-8} e \cdot cm$, the transition frequency $\omega_0 = 2\pi \cdot 508.333{\rm THz}$ (also equal the carrier frequency of the pulse, since resonance is assumed throughout the whole paper) and the decay constant $\Gamma_{\rm tot} = 61.542 \cdot 10^6 {\rm s}^{-1}$ corresponding to a lifetime $1/\Gamma_{\rm tot} = 16.249{\rm ns}$. We compute the value of $\mathcal{A}(\bar{\omega})$ by considering the transverse quantisation area to be proportional to the effective scattering of the light $\sigma \propto \lambda_0^2/2\pi$,

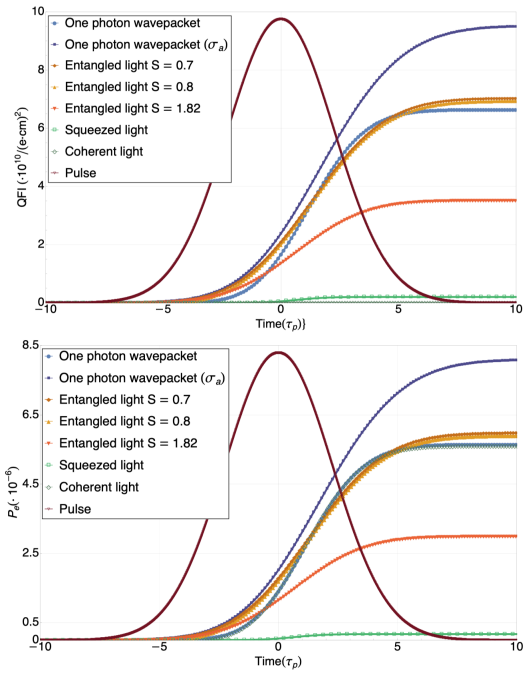

Figure 7. QFI and excitation probability for different states

with λ_0 the central wavelength of the light. With these parameter values, we obtain the ratio $\Gamma_\perp/\Gamma = 11.56$,[@Eva: please double check] similar to the value previously considered in Sec. (III); the decay rate into the perpendicular modes is obtained by subtracting the decay rate into the propagating pulse modes from the total free-space decay rate $\Gamma_\perp = \Gamma_{\rm tot} - \Gamma$. [This was not originally done in Eva's thesis/paper. She was considering $\Gamma_\perp = \Gamma_{\rm tot}$, using my notation. I think it must be done to be consistent though.]

We consider here an ultrashort Gaussian pulse with $T = 0.15$ps, which puts us well into the short-pulse regime defined previously: $T\Gamma_{\rm tot} = 9.2313 \cdot 10^{-6}$ and $T\Gamma = 7.34995 \cdot 10^{-7}$[@Eva: please double check this too] and we can thus neglect all spontaneous emission effects by considering the dynamics of the system up to shortly after the interaction, and employ the results of Sec. IV. This is also the reason why we can neglect the fact that $\Gamma_\perp$ is also proportional to μ^2; in this regime this contribution is totally negligible[8]

VII. DISCUSSION AND CONCLUSIONS

In this work we have studied a paradigmatic problem in quantum spectroscopy, the estimation of the dipole moment of a two-level atom, with the tools of quantum estimation theory and quantum metrology. We have employed fully quantum model of light-matter interaction, considering propagating pulses of quantum light. Even for the simplest quantum system, a two-level atom, the theoretical description of the evolution of the light is rather involved, since both the quantum state and the modal structure are affected by the interaction. From the perspective of quantum estimation theory we have highlighted that different sources of information about the parameter.

[Add summary of the results]

An important assumption we have made in this work is that the pulses are perfectly resonant, i.e. the carrier frequency is identical to the transition frequency of the two-level atom. Going beyond this assumption is possible, but warrants a more detailed discussion, since the problem is closely connected to the related problem of estimating the transition frequency of the atom. However, we have preliminary results showing that the resonant case is indeed the most advantageous for atomic and molecular [is this correct @Aiman?] parameter estimation [65, 66]

To conclude, this work is a first step towards the timely goal of understanding quantum spectroscopy more deeply thanks to rigorous precision bounds from estimation theory. In the future it will be important to extend this analysis to molecular systems that also undergo a non-Markovian dynamics due to the presence of a phononic bath, see e.g. [25].

Acknowledgements: This work was supported, in part, by a EPSRC New Horizons grant (EP/V04818X/1). EB was supported by the UK Quantum Technology Hub in Quantum Enhanced Imaging - QuantIC (EP/M01326X/1) and AK by a Chancellor's International Scholarship from the University of Warwick. Computing facilities were provided by the Scientific Computing Research Technology Platform of the University of Warwick.

[1] S. Mukamel, M. Freyberger, W. Schleich, M. Bellini, A. Zavatta, G. Leuchs, C. Silberhorn, R. W. Boyd, L. L. Sánchez-Soto, A. Stefanov, M. Barbieri, A. Paterova, L. Krivitsky, S. Shwartz, K. Tamasaku, K. Dorfman, F. Schlawin, V. Sandoghdar, M. G. Raymer, A. Marcus, O. Varnavski, T. Goodson, Z.-Y. Zhou, B.-S. Shi, S. Asban, M. O. Scully, G. S. Agarwal, T. Peng, A. V. Sokolov, Z.-D. Zhang, M. S. Zubairy, I. A. Vartanyants, E. del Valle, and F. Laussy, Roadmap on quantum light spectroscopy, J. Phys. B **53**, 072002 (2020).

[2] I. A. Walmsley, Quantum optics: Science and technology in a new light, Science (2015).

[3] K. E. Dorfman, F. Schlawin, and S. Mukamel, Nonlinear optical signals and spectroscopy with quantum light, Rev.

[8] When the effect of spontaneous emission is relevant and the atom is not perfectly coupled to the pulse, the problem of estimating μ is indeed sligthly different from estimating Γ.

Mod. Phys. **88**, 045008 (2016).
[4] A. Yabushita and T. Kobayashi, Spectroscopy by frequency-entangled photon pairs, Phys. Rev. A **69**, 013806 (2004).
[5] M. G. Raymer, A. H. Marcus, J. R. Widom, and D. L. P. Vitullo, Entangled Photon-Pair Two-Dimensional Fluorescence Spectroscopy (EPP-2DFS), J. Phys. Chem. B **117**, 15559 (2013).
[6] V. Giovannetti, S. Lloyd, and L. Maccone, Advances in quantum metrology, Nat. Photonics **5**, 222 (2011).
[7] E. Polino, M. Valeri, N. Spagnolo, and F. Sciarrino, Photonic quantum metrology, AVS Quantum Sci. **2**, 024703 (2020).
[8] M. Stobińska, G. Alber, and G. Leuchs, Chapter 8 - Quantum Electrodynamics of One-Photon Wave Packets, in *Advances in Quantum Chemistry*, Unstable States in the Continuous Spectra, Part I: Analysis, Concepts, Methods, and Results, Vol. 60, edited by C. A. Nicolaides and E. Brändas (Academic Press, 2010) pp. 457–483.
[9] Y. Wang, J. Minář, L. Sheridan, and V. Scarani, Efficient excitation of a two-level atom by a single photon in a propagating mode, Phys. Rev. A **83**, 063842 (2011).
[10] R. Whittaker, C. Erven, A. Neville, M. Berry, J. L. O'Brien, H. Cable, and J. C. F. Matthews, Absorption spectroscopy at the ultimate quantum limit from single-photon states, New J. Phys. **19**, 023013 (2017).
[11] C. S. Mitchell and M. P. Backlund, Quantum limits to resolution and discrimination of spontaneous emission lifetimes, Phys. Rev. A **105**, 062603 (2022).
[12] F. Schlawin, *Quantum-Enhanced Nonlinear Spectroscopy* (Springer International Publishing, Cham, 2017).
[13] H. T. Dinani, M. K. Gupta, J. P. Dowling, and D. W. Berry, Quantum-enhanced spectroscopy with entangled multiphoton states, Phys. Rev. A **93**, 063804 (2016).
[14] P. M. Birchall, E. J. Allen, T. M. Stace, J. L. O'Brien, J. C. F. Matthews, and H. Cable, Quantum Optical Metrology of Correlated Phase and Loss, Phys. Rev. Lett. **124**, 140501 (2020).
[15] J. Biele, S. Wollmann, J. W. Silverstone, J. C. F. Matthews, and E. J. Allen, Maximizing precision in saturation-limited absorption measurements, Phys. Rev. A **104**, 053717 (2021).
[16] A. Stefanov, On the role of entanglement in two-photon metrology, Quantum Sci. Technol. **2**, 025004 (2017).
[17] G. Adesso, F. Dell'Anno, S. De Siena, F. Illuminati, and L. A. M. Souza, Optimal estimation of losses at the ultimate quantum limit with non-Gaussian states, Phys. Rev. A **79**, 040305(R) (2009).
[18] R. Nair, Quantum-Limited Loss Sensing: Multiparameter Estimation and Bures Distance between Loss Channels, Phys. Rev. Lett. **121**, 230801 (2018).
[19] K. J. Blow, R. Loudon, S. J. D. Phoenix, and T. J. Shepherd, Continuum fields in quantum optics, Phys. Rev. A **42**, 4102 (1990).
[20] M. Scully and M. S. Zubairy, *Quantum Optics* (Cambridge University Press, 1997).
[21] C. W. Gardiner and P. Zoller, *Quantum Noise: A Handbook of Markovian and Non-Markovian Quantum Stochastic Methods with Applications to Quantum Optics* (Springer, 2004).
[22] K. R. Parthasarathy, *An Introduction to Quantum Stochastic Calculus* (Birkhäuser Basel, Basel, 1992).
[23] B. Q. Baragiola, *Open Systems Dynamics for Propagating Quantum Fields*, Ph.D. thesis (2014), arXiv:1408.4447.
[24] K. A. Fischer, Exact calculation of stimulated emission driven by pulsed light, OSA Continuum, OSAC **1**, 772 (2018).
[25] L. Ko, R. L. Cook, and K. B. Whaley, Dynamics of photosynthetic light harvesting systems interacting with N-photon Fock states, J. Chem. Phys. , (in press) (2022).
[26] A. Silberfarb and I. H. Deutsch, Entanglement generated between a single atom and a laser pulse, Phys. Rev. A **69**, 042308 (2004).
[27] A. Silberfarb and I. H. Deutsch, Continuous measurement with traveling-wave probes, Phys. Rev. A **68**, 013817 (2003).
[28] W. Konyk and J. Gea-Banacloche, Quantum multimode treatment of light scattering by an atom in a waveguide, Phys. Rev. A **93**, 063807 (2016).
[29] A. Roulet and V. Scarani, Solving the scattering of N photons on a two-level atom without computation, New J. Phys. **18**, 093035 (2016).
[30] A. Dąbrowska, D. Chruściński, S. Chakraborty, and G. Sarbicki, Eternally non-Markovian dynamics of a qubit interacting with a single-photon wavepacket, New J. Phys. **23**, 123019 (2021).
[31] B. Q. Baragiola, R. L. Cook, A. M. Brańczyk, and J. Combes, N-photon wave packets interacting with an arbitrary quantum system, Phys. Rev. A **86**, 013811 (2012).
[32] J. A. Gross, B. Q. Baragiola, T. M. Stace, and J. Combes, Master equations and quantum trajectories for squeezed wave packets, Phys. Rev. A **105**, 023721 (2022).
[33] A. H. Kiilerich and K. Mølmer, Input-Output Theory with Quantum Pulses, Phys. Rev. Lett. **123**, 123604 (2019).
[34] A. H. Kiilerich and K. Mølmer, Quantum interactions with pulses of radiation, Phys. Rev. A **102**, 023717 (2020).
[35] B. Brecht, D. V. Reddy, C. Silberhorn, and M. G. Raymer, Photon Temporal Modes: A Complete Framework for Quantum Information Science, Phys. Rev. X **5**, 041017 (2015).
[36] M. G. Raymer and I. A. Walmsley, Temporal modes in quantum optics: Then and now, Phys. Scr. **95**, 064002 (2020).
[37] C. Fabre and N. Treps, Modes and states in quantum optics, Rev. Mod. Phys. **92**, 035005 (2020).
[38] M. A. Nielsen and I. L. Chuang, *Quantum Computation and Quantum Information*, 10th ed. (Cambridge University Press, Cambridge New York, 2010).
[39] T. M. Cover and J. A. Thomas, *Elements of Information Theory*, 2nd ed. (Wiley-Interscience, 2006).
[40] H. L. Van Trees, K. L. Bell, and Z. Tian, *Detection Estimation and Modulation Theory*, second edition ed., Vol. Volume 1. Detection, estimation, and filtering theory (John Wiley & Sons, Inc, Hoboken, N.J, 2013).
[41] C. W. Helstrom, *Quantum Detection and Estimation Theory* (Academic Press, New York, 1976).
[42] A. S. Holevo, *Probabilistic and Statistical Aspects of Quantum Theory*, 2nd ed. (Edizioni della Normale, Pisa, 2011).
[43] S. L. Braunstein and C. M. Caves, Statistical distance and the geometry of quantum states, Phys. Rev. Lett. **72**, 3439 (1994).
[44] M. G. A. Paris, Quantum estimation for quantum technology, Int. J. Quantum Inf. **07**, 125 (2009).
[45] M. G. Genoni and T. Tufarelli, Non-orthogonal bases for quantum metrology, J. Phys. Math. Theor. **52**, 434002 (2019).
[46] E. Bisketzi, D. Branford, and A. Datta, Quantum limits of

localisation microscopy, New J. Phys. **21**, 123032 (2019).
[47] L. J. Fiderer, T. Tufarelli, S. Piano, and G. Adesso, General Expressions for the Quantum Fisher Information Matrix with Applications to Discrete Quantum Imaging, PRX Quantum **2**, 020308 (2021).
[48] S. Alipour and A. T. Rezakhani, Extended convexity of quantum Fisher information in quantum metrology, Phys. Rev. A **91**, 042104 (2015).
[49] S. Ng, S. Z. Ang, T. A. Wheatley, H. Yonezawa, A. Furusawa, E. H. Huntington, and M. Tsang, Spectrum analysis with quantum dynamical systems, Phys. Rev. A **93**, 042121 (2016).
[50] T. Shitara, Y. Kuramochi, and M. Ueda, Trade-off relation between information and disturbance in quantum measurement, Phys. Rev. A **93**, 032134 (2016).
[51] J. Combes, C. Ferrie, Z. Jiang, and C. M. Caves, Quantum limits on postselected, probabilistic quantum metrology, Phys. Rev. A **89**, 052117 (2014).
[52] P. Farrera, G. Heinze, B. Albrecht, M. Ho, M. Chávez, C. Teo, N. Sangouard, and H. de Riedmatten, Generation of single photons with highly tunable wave shape from a cold atomic ensemble, Nat Commun **7**, 13556 (2016).
[53] O. Morin, M. Körber, S. Langenfeld, and G. Rempe, Deterministic Shaping and Reshaping of Single-Photon Temporal Wave Functions, Phys. Rev. Lett. **123**, 133602 (2019).
[54] M. Karpiński, A. O. C. Davis, F. Sośnicki, V. Thiel, and B. J. Smith, Control and Measurement of Quantum Light Pulses for Quantum Information Science and Technology, Adv. Quantum Technol. **4**, 2000150 (2021).
[55] M. Lipka and M. Parniak, Single-Photon Hologram of a Zero-Area Pulse, Phys. Rev. Lett. **127**, 163601 (2021).
[56] H. S. Rag and J. Gea-Banacloche, Two-level-atom excitation probability for single- and N -photon wave packets, Phys. Rev. A **96**, 033817 (2017).
[57] J. Larson and T. Mavrogordatos, *The Jaynes–Cummings Model and Its Descendants* (IOP Publishing, Bristol, UK, 2021).
[58] E. Bisketzi, *Quantum Limits in Microscopy and Spectroscopy*, Ph.D. thesis, University of Warwick (2022).
[59] V. R. Christiansen, A. H. Kiilerich, and K. Mølmer, Interaction of quantum systems with single pulses of quantized radiation, arXiv:2203.07477 (2022).
[60] M. G. Genoni and C. Invernizzi, Optimal quantum estimation of the coupling constant of Jaynes-Cummings interaction, Eur. Phys. J. Spec. Top. **203**, 49 (2012).
[61] A. Monras and M. G. A. Paris, Optimal Quantum Estimation of Loss in Bosonic Channels, Phys. Rev. Lett. **98**, 160401 (2007).
[62] F. Schlawin, Entangled photon spectroscopy, J. Phys. B At. Mol. Opt. Phys. **50**, 203001 (2017).
[63] R. Demkowicz-Dobrzański and L. Maccone, Using Entanglement Against Noise in Quantum Metrology, Phys. Rev. Lett. **113**, 250801 (2014).
[64] D. Layden, S. Zhou, P. Cappellaro, and L. Jiang, Ancilla-Free Quantum Error Correction Codes for Quantum Metrology, Phys. Rev. Lett. **122**, 040502 (2019).
[65] A. Khan, ..., Ph.D. thesis, University of Warwick (2022).
[66] A. Khan, E. Bisketzi, F. Albarelli, and A. Datta, In preparation (2022).
[67] W. P. Grice, A. B. U'Ren, and I. A. Walmsley, Eliminating frequency and space-time correlations in multiphoton states, Phys. Rev. A **64**, 063815 (2001).
[68] S. Parker, S. Bose, and M. B. Plenio, Entanglement quantification and purification in continuous-variable systems, Phys. Rev. A **61**, 032305 (2000).
[69] L. Lamata and J. León, Dealing with entanglement of continuous variables: Schmidt decomposition with discrete sets of orthogonal functions, J. Opt. B: Quantum Semiclass. Opt. **7**, 224 (2005).
[70] C. K. Law, I. A. Walmsley, and J. H. Eberly, Continuous Frequency Entanglement: Effective Finite Hilbert Space and Entropy Control, Phys. Rev. Lett. **84**, 5304 (2000).
[71] D. A. Steck, Sodium D Line Data (2019).

Appendix A: Equivalence between spontaneous emission into many modes or a single mode

[This Appendix is probably not really needed, but I originally wrote it to convince myself the model was appropriate and equivalent to [25].] Let us keep it for completeness.

A two-level atom in free space can be described as interacting with a discrete set of infinitely many modes of the electromagnetic field. With the usual dipole and Markovian approximations (explained in the main text) the interaction-picture Hamiltonian is

$$\begin{aligned} H_{\mathrm{I}}(t) = &- \mathrm{i}\sqrt{\Gamma_{\mathrm{tot}}\eta_P}\big(\sigma_- a(t)^\dagger - \sigma_+ a^\dagger(t)\big) \\ &- \mathrm{i}\sum_j \sqrt{\Gamma_{\mathrm{tot}}\eta_j}\Big(\sigma_- a_j(t) - \sigma_+ a_j^\dagger(t)\Big). \end{aligned} \tag{A1}$$

In this expression Γ_{tot} is the standard Wigner-Weisskopf spontaneous-emission rate in free space, which could be suitably modified to model emission of radiation in a different propagating medium, while the parameters $\eta_l > 0$ are geometric factors that determine the coupling of the atom with the mode l, see for instance Ref. [25] for a more in-depth discussion. In particular, we have separated the term corresponding to the interaction with the travelling pulse mode, which we assume to be the only experimentally accessible one. The others modes are initially in the vacuum and we treat them as an inaccessible, i.e. the environment degrees of freedom. For this reason, it is more convenient to treat them as a single collective mode, defined as

$$b(t) = \sum_j \sqrt{\frac{\eta_j}{\sum_{j'}\eta_{j'}}}\, a_j(t), \tag{A2}$$

and satisfying $[b(t), b^\dagger(t')] = \delta(t-t')$ so that we can rewrite the Hamiltonian (7) used in the main text with $\Gamma = \Gamma_{\rm tot}\eta_P$ and $\Gamma_\perp = \Gamma_{\rm tot}\sum_j \eta_j$.

Appendix B: QFI of a rank-2 state

We consider the rank-2 density matrix

$$\rho_\mu = \left|\tilde\psi_e\right\rangle\!\left\langle\tilde\psi_e\right| + \left|\tilde\psi_g\right\rangle\!\left\langle\tilde\psi_g\right|, \tag{B1}$$

and we denote with $\mathcal{B}$ the (generally nonorthogonal) basis formed by these two vectors and their derivatives

$$\mathcal{B} = \{\left|\tilde\psi_e\right\rangle, \left|\tilde\psi_g\right\rangle, \left|\partial_\mu\tilde\psi_e\right\rangle, \left|\partial_\mu\tilde\psi_g\right\rangle\}. \tag{B2}$$

with the following Gramiam matrix

$$G^{\mathcal{B}} = \begin{bmatrix} \langle\tilde\psi_e|\tilde\psi_e\rangle & \langle\tilde\psi_e|\tilde\psi_g\rangle & \langle\tilde\psi_e|\partial_\Gamma\tilde\psi_e\rangle & \langle\tilde\psi_e|\partial_\Gamma\tilde\psi_g\rangle \\ \langle\tilde\psi_g|\tilde\psi_e\rangle & \langle\tilde\psi_g|\tilde\psi_g\rangle & \langle\tilde\psi_g|\partial_\Gamma\tilde\psi_e\rangle & \langle\tilde\psi_g|\partial_\Gamma\tilde\psi_g\rangle \\ \langle\partial_\Gamma\tilde\psi_e|\tilde\psi_e\rangle & \langle\partial_\Gamma\tilde\psi_e|\tilde\psi_g\rangle & \langle\partial_\Gamma\tilde\psi_e|\partial_\Gamma\tilde\psi_e\rangle & \langle\partial_\Gamma\tilde\psi_e|\partial_\Gamma\tilde\psi_g\rangle \\ \langle\partial_\Gamma\tilde\psi_g|\tilde\psi_e\rangle & \langle\partial_\Gamma\tilde\psi_g|\tilde\psi_g\rangle & \langle\partial_\Gamma\tilde\psi_g|\partial_\Gamma\tilde\psi_e\rangle & \langle\partial_\Gamma\tilde\psi_g|\partial_\Gamma\tilde\psi_g\rangle \end{bmatrix}. \tag{B3}$$

Assuming that $\mathcal{B}$ is a basis means that the vectors must be linearly independent and thus $G^{\mathcal{B}}$ invertible. While the linear independence of $|\psi_e\rangle$ and $|\psi_g\rangle$ is implied by the assumption that ρ_Γ is rank-2, the linear independence of the whole basis $\mathcal{B}$ is as an extra assumption in this derivation, but it is valid for the applications considered in this paper.

Using the notation of Ref. [47] we can represent operators as matrices expressed on the basis $\mathcal{B}$ and Eq. (21) becomes

$$2\partial_\Gamma\rho^{\mathcal{B}} = L_\Gamma^{\mathcal{B}} G_\Gamma^{\mathcal{B}}\rho_\Gamma^{\mathcal{B}} + \rho_\Gamma^{\mathcal{B}} G_\Gamma^{\mathcal{B}} L_\Gamma^{\mathcal{B}}. \tag{B4}$$

This equation can be solved efficiently by using block vectorization [46, 47]. Once a solution is found, the QFI can be evaluated as

$$\mathcal{Q}(\rho_\Gamma) = \mathrm{Tr}\left[L_\Gamma^{\mathcal{B}} G^{\mathcal{B}}\partial_\Gamma\rho_\Gamma^{\mathcal{B}} G^{\mathcal{B}}\right] \tag{B5}$$

For this particular problem??? Refer to Eqn./Sec in main text. the density matrix and its derivative have a very simple form

$$\rho^{\mathcal{B}} = \begin{bmatrix} 1&0&0&0\\0&1&0&0\\0&0&0&0\\0&0&0&0\end{bmatrix} \qquad \partial_\Gamma\rho^{\mathcal{B}} = \begin{bmatrix} 0&0&1&0\\0&0&0&1\\1&0&0&0\\0&1&0&0\end{bmatrix} \tag{B6}$$

and the Lyapunov equation can be solved analytically to obtain an explicit, albeit complicated, expression for the QFI that depends only on the matrix elements of $G^{\mathcal{B}}$.

$$\begin{aligned}\mathcal{Q}(\rho_\Gamma) =& \frac{-4}{\Delta(G_{11}+G_{22})}\Big\{\Delta\left[(\mathrm{Im}\,G_{13}-\mathrm{Im}\,G_{24})^2+(\mathrm{Im}\,G_{14}+\mathrm{Im}\,G_{23})^2\right] \\ &+4\Delta G_{11}(\mathrm{Im}\,G_{33}+\mathrm{Im}\,G_{44})+4\Delta G_{22}(\mathrm{Im}\,G_{33}+\mathrm{Im}\,G_{44}) \\ &-4(\mathrm{Im}\,G_{13})^2G_{22}^2+8\,\mathrm{Im}\,G_{13}\,\mathrm{Re}\,G_{12}G_{22}(\mathrm{Im}\,G_{14}+\mathrm{Im}\,G_{23})+8\,\mathrm{Im}\,G_{13}\,\mathrm{Im}\,G_{12}G_{22}(\mathrm{Re}\,G_{23}-\mathrm{Re}\,G_{14}) \\ &-4G_{11}G_{22}\left[2\,\mathrm{Im}\,G_{13}\,\mathrm{Im}\,G_{24}+(\mathrm{Re}\,G_{14}-\mathrm{Re}\,G_{23})^2\right]+8\,\mathrm{Im}\,G_{12}\,\mathrm{Re}\,G_{12}(\mathrm{Im}\,G_{14}+\mathrm{Im}\,G_{23})(\mathrm{Re}\,G_{14}-\mathrm{Re}\,G_{23}) \\ &+8\,\mathrm{Im}\,G_{24}\,\mathrm{Re}\,G_{12}G_{11}(\mathrm{Im}\,G_{14}+\mathrm{Im}\,G_{23}) \\ &-4(\mathrm{Re}\,G_{12})^2(\mathrm{Im}\,G_{14}+\mathrm{Im}\,G_{23}+\mathrm{Re}\,G_{14}-\mathrm{Re}\,G_{23})(\mathrm{Im}\,G_{14}+\mathrm{Im}\,G_{23}-\mathrm{Re}\,G_{14}+\mathrm{Re}\,G_{23}) \\ &+8\,\mathrm{Im}\,G_{12}\,\mathrm{Im}\,G_{24}G_{11}(\mathrm{Re}\,G_{23}-\mathrm{Re}\,G_{14})-4(\mathrm{Im}\,G_{24})^2G_{11}^2\Big\},\end{aligned}$$

where $\Delta = G_{11}G_{22}-|G_{12}|^2 > 0$ is the determinant of the first diagonal block of $G^{\mathcal{B}}$ and the superscript $\mathcal{B}$ has been suppressed for compactness. Where is this used in the main text?

Appendix C: Explicit check of single photon states normalization

As in the rest of the manuscript we assume real valued pulse amplitudes $\xi(t')$ so that we deal with real wavefunctions. Here we consider the case $\Gamma_\perp = 0$ for simplicity. The amplitude of the excited atomic state is

$$\psi_e(t) = -\sqrt{\Gamma}\int_{-\infty}^{t} dt' e^{-\frac{\Gamma}{2}(t-t')}\xi(t') \tag{C1}$$

and the corresponding probability is

$$\psi_e(t)^2 = \Gamma\left(\int_{-\infty}^{t} dt' e^{-\frac{\Gamma}{2}(t-t')}\xi(t')\right)^2 = \Gamma e^{-\Gamma t}\left(\int_{-\infty}^{t} dt' e^{\frac{\Gamma}{2}t'}\xi(t')\right)^2. \tag{C2}$$

The pulse component is

$$|\psi_{g,P}(t)\rangle = \int_{-\infty}^{\infty} d\tau\Big(\xi(\tau) + \sqrt{\Gamma}\Theta(t-\tau)\psi_e(\tau)\Big)a_P^\dagger(\tau)|0_P\rangle \tag{C3}$$

with modulus squared

$$\begin{aligned}
\langle\psi_g(t)|\psi_g(t)\rangle &= \int_{-\infty}^{\infty} d\tau\Big(\xi(\tau) + \sqrt{\Gamma}\Theta(t-\tau)\psi_e(\tau)\Big)^2 \\
&= \int_{-\infty}^{\infty} d\tau\xi(\tau)^2 + \int_{-\infty}^{t} d\tau\Big(\Gamma\psi_e(\tau)^2 + 2\sqrt{\Gamma}\psi_e(\tau)\xi(\tau)\Big) \\
&= 1 + \Gamma^2\int_{-\infty}^{t} d\tau\left(\int_{-\infty}^{\tau} dt' e^{-\frac{\Gamma}{2}(\tau-t')}\xi(t')\right)^2 - 2\Gamma\int_{-\infty}^{t} d\tau\left(\int_{-\infty}^{\tau} dt' e^{-\frac{\Gamma}{2}(\tau-t')}\xi(t')\right)\xi(\tau).
\end{aligned} \tag{C4}$$

We now show that the two terms except the unity equals $-\psi_e(t)^2$ by recognizing a derivative inside the integral.

$$\begin{aligned}
&\Gamma^2\int_{-\infty}^{t} d\tau\left(\int_{-\infty}^{\tau} dt' e^{-\frac{\Gamma}{2}(\tau-t')}\xi(t')\right)^2 - 2\Gamma\int_{-\infty}^{t} d\tau\left(\int_{-\infty}^{\tau} dt' e^{-\frac{\Gamma}{2}(\tau-t')}\xi(t')\right)\xi(\tau) \\
=&\Gamma\int_{-\infty}^{t} d\tau\left[\Gamma e^{-\Gamma\tau}\left(\int_{-\infty}^{\tau} dt' e^{\frac{\Gamma}{t}'}\xi(t')\right)^2 - 2e^{-\frac{\Gamma}{2}\tau}\left(\int_{-\infty}^{\tau} dt' e^{\frac{\Gamma}{2}t'}\xi(t')\right)\xi(\tau)\right] \\
=&\Gamma\int_{-\infty}^{t} d\tau\left[\Gamma e^{-\Gamma\tau}\left(\int_{-\infty}^{\tau} dt' e^{\frac{\Gamma}{t}'}\xi(t')\right)^2 - e^{-\Gamma t}\frac{d}{d\tau}\left(\int_{-\infty}^{\tau} dt' e^{\frac{\Gamma}{2}t'}\xi(t')\right)^2\right] \\
=&-\Gamma\int_{-\infty}^{t} d\tau\frac{d}{d\tau}\left[e^{-\Gamma\tau}\left(\int_{-\infty}^{\tau} dt' e^{\frac{\Gamma}{2}t'}\xi(t')\right)^2\right] = -\Gamma e^{-\Gamma t}\left(\int_{-\infty}^{t} dt' e^{\frac{\Gamma}{2}t'}\xi(t')\right)^2.
\end{aligned} \tag{C5}$$

The reasoning when $\Gamma_\perp > 0$ is completely analogous.

Appendix D: Single-photon QFI

We can rewrite the QFI in terms of the unnormalized state $\left|\tilde{\psi}_\Gamma\right\rangle = \sqrt{1-p_\Gamma}|\psi_\Gamma\rangle$, satisfying $\left\langle\tilde{\psi}_\Gamma\middle|\tilde{\psi}_\Gamma\right\rangle = 1-p_\Gamma$ and $|\partial_\Gamma\psi_\Gamma\rangle = \frac{1}{\sqrt{1-p_\Gamma}}\left|\partial_\Gamma\tilde{\psi}_\Gamma\right\rangle + \frac{\partial_\Gamma p_\Gamma}{2(1-p_\Gamma)^{3/2}}\left|\tilde{\psi}_\Gamma\right\rangle$ and substituting this expression in the third term of (31) we obtain an alternative expression for the QFI

$$\mathcal{Q}_\Gamma = (\partial_\Gamma p_\Gamma)^2/p_\Gamma + 4\left\langle\partial_\Gamma\tilde{\psi}_\Gamma\middle|\partial_\Gamma\tilde{\psi}_\Gamma\right\rangle \tag{D1}$$

where the equivalence holds because

$$\left\langle\partial_\Gamma\tilde{\psi}_\Gamma\middle|\partial_\Gamma\tilde{\psi}_\Gamma\right\rangle = (1-p_\Gamma)\langle\partial_\Gamma\psi_\Gamma|\partial_\Gamma\psi_\Gamma\rangle + \frac{(\partial_\Gamma p_\Gamma)^2}{4(1-p_\Gamma)} \tag{D2}$$

The form in Eq. (D1) is particularly convenient, since we can immediately use the unnormalized state (27) without renormalizing it first. These identities hold because we have $\langle\psi|\partial_\Gamma\psi\rangle = 0$.

The terms appearing in (D1) can be evaluated more explicitly as follows (we use the notation $\|v\|^2 = \langle v|v\rangle$)

$$p_\Gamma(t) = \psi_e(t)^2 + \|\psi_{g,E}(t)\|^2 \tag{D3}$$

$$\psi_e(t)^2 = \Gamma\left(\int_{-\infty}^{t} dt' e^{-\frac{\Gamma+\Gamma_\perp}{2}(t-t')}\xi(t')\right)^2 \tag{D4}$$

$$\|\psi_{g,E}(t)\|^2 = \Gamma_\perp\Gamma\int_{-\infty}^{t} d\tau\left(\int_{-\infty}^{\tau} dt' e^{-\frac{\Gamma+\Gamma_\perp}{2}(\tau-t')}\xi(t')\right)^2 \tag{D5}$$

$$\begin{aligned}\partial_\Gamma p_\Gamma(t) = &\left(\int_{-\infty}^{t} dt' e^{-\frac{\Gamma+\Gamma_\perp}{2}(t-t')}\xi(t')\right)^2 + 2\Gamma\left(\int_{-\infty}^{t} dt' e^{-\frac{\Gamma+\Gamma_\perp}{2}(t-t')}\xi(t')\right)\left(\int_{-\infty}^{t} dt' \frac{(t'-t)}{2} e^{-\frac{\Gamma+\Gamma_\perp}{2}(t-t')}\xi(t')\right)\\ &+\Gamma_\perp\int_{-\infty}^{t} d\tau\left(\int_{-\infty}^{\tau} dt' e^{-\frac{\Gamma+\Gamma_\perp}{2}(\tau-t')}\xi(t')\right)^2\\ &+2\Gamma_\perp\Gamma\int_{-\infty}^{t} d\tau\left(\int_{-\infty}^{\tau} dt' e^{-\frac{\Gamma+\Gamma_\perp}{2}(\tau-t')}\xi(t')\right)\left(\int_{-\infty}^{\tau} dt' \frac{t'-\tau}{2} e^{-\frac{\Gamma+\Gamma_\perp}{2}(\tau-t')}\xi(t')\right)\end{aligned} \tag{D6}$$

$$\begin{aligned}\left\|\partial_\Gamma\tilde{\psi}_{g,P}\right\|^2 = &\int_{-\infty}^{t} d\tau\left(\int_{-\infty}^{\tau} dt' e^{-\frac{\Gamma+\Gamma_\perp}{2}(\tau-t')}\xi(t')\right)^2 + \Gamma^2\int_{-\infty}^{t} d\tau\left(\int_{-\infty}^{\tau} dt' \frac{(t'-\tau)}{2} e^{-\frac{\Gamma+\Gamma_\perp}{2}(\tau-t')}\xi(t')\right)^2\\ &+2\Gamma\int_{-\infty}^{t} d\tau\left(\int_{-\infty}^{\tau} dt' e^{-\frac{\Gamma+\Gamma_\perp}{2}(\tau-t')}\xi(t')\right)\left(\int_{-\infty}^{\tau} dt' \frac{(t'-\tau)}{2} e^{-\frac{\Gamma+\Gamma_\perp}{2}(\tau-t')}\xi(t')\right).\end{aligned} \tag{D7}$$

Appendix E: Single-photon wavepackets details

In Table I we report details for all the pulse shapes mentioned in Figs. 2 and 3, including the definition, the excitation probability the QSNR and the SNR corresponding to a measurement in the original temporal mode; as mentioned in the main text the relevant parameter for these quantities is the dimensionless product ΓT. For the Gaussian pulse analytical expressions for the QFI are not available. The arrival time of all the pulses corresponds to their peak, except for the rectangular pulse for which it corresponds to the beginning of the nonzero region.

Table I. Pulse shapes used in the main text. The arrival of all the pulses is at $t = 0$. Θ is the Heaviside step function.

Shape	$\xi(t)$	$\xi(t)^2$-st. dev.	$p_e(t)$	$\Gamma^2\mathcal{Q}(\rho_\Gamma^\infty)$	$\Gamma^2\mathcal{C}(p_{\text{orig}})$
Rectangular	$\frac{\Theta(t)\Theta(T-t)}{\sqrt{T}}$	$\frac{T}{\sqrt{12}}$	$\frac{4e^{-\Gamma t}\left(e^{\frac{\Gamma t}{2}}-1\right)^2}{\Gamma T}$	$\frac{8\left(2-e^{-\frac{\Gamma T}{2}}(\Gamma T+2)\right)}{\Gamma T}$	$\frac{2\left(\Gamma T-2e^{\frac{\Gamma T}{2}}+2\right)^2}{\left(e^{\frac{\Gamma T}{2}}-1\right)\left(e^{\frac{\Gamma T}{2}}(\Gamma T-2)+2\right)}$
Rising Exp	$\frac{1}{\sqrt{T}}e^{\frac{t}{2T}}\Theta(-t)$	T	$\frac{4\Gamma T e^{-\Gamma t}}{(\Gamma T+1)^2}\Theta(t)$	$\frac{8\Gamma T}{(\Gamma T+1)^2}$	$\frac{4\Gamma T}{(\Gamma T+1)^2}$
Decaying Exp	$\frac{1}{\sqrt{T}}e^{-\frac{t}{2T}}\Theta(t)$	T	$\frac{4\Gamma T e^{-\Gamma t}\left(e^{\frac{t(\Gamma T-1)}{2T}}-1\right)^2}{(\Gamma T-1)^2}$	$\frac{8\Gamma T}{(\Gamma T+1)^2}$	$\frac{4\Gamma T}{(\Gamma T+1)^2}$
Symmetric Exp	$\frac{1}{\sqrt{T}}e^{-\frac{\lvert t\rvert}{T}}$	T	$\begin{cases}\frac{4\Gamma T e^{\frac{2t}{T}}}{(\Gamma T+2)^2} & t\le 0\\ \frac{4\Gamma T e^{-\Gamma t}\left((\Gamma T+2)e^{\frac{1}{2}t\left(\Gamma-\frac{2}{T}\right)}-4\right)^2}{\left[(\Gamma T)^2-4\right]^2} & t>0\end{cases}$	$\frac{64\Gamma T}{(\Gamma T+2)^3}$	$\frac{64\Gamma T}{(\Gamma T+2)^2(\Gamma T+4)}$
Gaussian	$\frac{1}{\sqrt{T}(2\pi)^{1/4}}e^{-\frac{t^2}{4T^2}}$	T	$\sqrt{\frac{\pi}{2}}\Gamma T e^{\frac{(\Gamma T)^2-2\Gamma t}{2}}\left(\text{erf}\left(\frac{t}{2T}-\frac{\Gamma T}{2}\right)+1\right)^2$	n.a.	n.a.